UPR-904-T,
CERN-TH/2000-270,
FERMILAB-Pub-00/257-T,
RUNHETC-2000-36,
SISSA-Ref.89/2000/EP
hep-th/yymmxxx

Discrete Wilson Lines in N=1 D=4 Type IIB Orientifolds: A Systematic Exploration for $\mathbf{Z_6}$ Orientifold

Mirjam Cvetič[1], Angel M. Uranga[2] and Jing Wang[3]

[1] *Dept. of Physics and Astronomy, Univ. of Pennsylvania, Philadelphia PA 19104-6396, USA; Dept. of Physics and Astronomy, Rutgers Univ., Piscataway, NJ 08855-0849, USA; SISSA-ISAS and INFN, Sezione di Trieste, Via Beirut 2-4, I-34013, Trieste, Italy*

[2] *Fermilab, Theory Division, Batavia, IL 60510, USA*

[3] *Theory Division, CERN, CH-1211 Geneva 23, Switzerland*

(February 1, 2008)

Abstract

We develop techniques to construct general discrete Wilson lines in four-dimensional N=1 Type IIB orientifolds, their T-dual realization corresponds to branes positioned at the orbifold fixed points. The explicit order two and three Wilson lines along with their tadpole consistency conditions are given for D=4 N=1 $\mathbf{Z_6}$ Type IIB orientifold. The systematic search for all models with general order three Wilson lines leads to a small class of inequivalent models. There are only two inequivalent classes of a potentially phenomenologically interesting model that has a possible $SU(3)_{color} \times SU(2)_L \times SU(2)_R \times U(1)_{B-L}$ gauge structure, arising from a set of branes located at the $\mathbf{Z_6}$ orbifold fixed point. We calculate the spectrum and Yukawa couplings for this model. On the other hand, introduction of anti-branes allows for models with three families and realistic gauge group assignment, arising from branes located at the $\mathbf{Z_3}$ orbifold fixed points.

I. INTRODUCTION

Four-dimensional N=1 supersymmetric Type IIB orientifolds ([1–9] and references therein) provide a fertile ground to study new physics implications of perturbative open-string theories which in turn could shed light on the physics of strongly coupled heterotic string models. In this effort one is at fairly early stages. One goal, that is far from being achieved, is the development of techniques that would yield a larger class of solutions (see e.g., [10] and references therein) than those based on symmetric orientifold constructions. Another direction is the exploration of possible deformations of symmetric orientifold models, which in turn may provide large new classes of models which may eventually lead to models with quasi-realistic features.

Such deformations fall into two classes: (i) Wilson lines, which in the T-dual picture correspond to branes moved to different positions on the orientifold, (ii) blow-up of orientifold singularities.

The deformations in the space of supersymmetric four-dimensional solutions have a field-theoretic realization; one identifies specific D- and F-flat directions within the effective theory of the original model [1]. The effective field theory at the new (deformed) supersymmetric ground states is a power-series in the magnitude of the vacuum expectation values of the fields responsible for the deformation. In particular, this technique was used to study the blowing-up of the orientifold singularities [2] [13,14], where the $\mathbf{Z_3}$ [1] and $\mathbf{Z_2} \times \mathbf{Z_2}$ N=1 D=4 orientifolds are used as prototypes. Results are different in nature from those of perturbative heterotic orbifolds [15]. The blowing-up deformation is notoriously difficult to describe within the full string theory context, since the metric of the blown-up space is not explicitly known. On the other hand the explicit field-theoretic realization in terms of (non-Abelian) flat directions allows for the determination of the surviving gauge groups and massless spectrum.

On the other hand Wilson lines, both continuous and discrete, can in principle be constructed within full string theory. The T-dual interpretation of continuous Wilson lines corresponds to a set of branes located at generic points on the orientifold, while discrete Wilson lines correspond to special cases of sets of branes located at the orbifold fixed points.

---

[1] Such techniques have been extensively applied to the studies of heterotic string models, see. e.g., [11] and references therein.

[2] Previous work on blowing up orbifold singularities has appeared in [12].

Deformation by continuous Wilson lines admits an interpretation in the effective field theory as specific D- and F-flat directions, which describe (in the T-dual picture) infinitesimal motion of sets of branes away from the fixed points.

Explicit examples of discrete Wilson lines have been constructed for a number of different orientifold models (see [6,8,9,16] and references therein). Continuous Wilson lines were first addressed in [5,6], but the explicit unitary representation was not given. The explicit unitary representation of the continuous Wilson line, specifically constructed for the $\mathbf{Z_3}$ orientifold, along with the most general set of continuous Wilson lines and their field theory realization for $\mathbf{Z_3}$ orientifold was recently given in [17].

The purpose of this paper is to advance the techniques to construct models with general discrete Wilson lines for general symmetric Type IIB orientifolds. In particular we construct the explicit form of such Wilson lines which satisfy both the algebraic consistency conditions and the tadpole consistency conditions. We carry out our discussion in the T-dual picture, where Wilson lines have a geometric interpretation as sets of branes located at different fixed points. Algebraic consistency conditions amount to the consistency of the location of these branes with the orbifold/orientifold symmetries. We also show that the T-dual tadpole consistency conditions are related to the original ones by a discrete Fourier transform. We apply these techniques to fully explore the $\mathbf{Z_6}$ orientifold model with a very general choice of discrete Wilson lines. However, we would like to emphasize the techniques are general, and apply to other orientifolds as well.

One of the motivations to study this particular model is that it could be very interesting from the phenomenological point of view, since it may allow for putting branes at $\mathbf{Z_3}$ *orbifold* points (that are not fixed under orientifold projection). The relevance of configurations of branes at $\mathbf{Z_3}$ orbifold points to obtain potentially realistic models has been discussed in [18]. If six branes are located at such points such sectors may provide standard model gauge groups with three families. However, we find the consistency constraints do not allow for the gauge structure $SU(3)_{color} \times SU(2)_L \times U(1)$ in such sectors. This is only possible if one includes anti-branes in the model and breaks supersymmetry (in a hidden sector).

Nevertheless we carry out a systematic exploration of all the possible models with N=1 supersymmetry and find a small class of inequivalent models. When restricting to models containing sectors with $SU(3)$ gauge group factors, as candidates for $SU(3)_{color}$, we find only two inequivalent classes, with a possible gauge group assignment $SU(3)_{color} \times SU(2)_L \times SU(2)_R \times U(1)_{B-L}$ that arises from branes located at the $\mathbf{Z_6}$ orbifold fixed point. We provide the full massless spectrum and the Yukawa couplings, thus setting the stage for

further phenomenological explorations of this model.

The paper is organized in the following way. In Section II we construct both order three (Subsection II A) and order two (Subsection II B) discrete Wilson lines for $\mathbf{Z_6}$ orientifold, as well as continuous Wilson lines (Subsection II C), and provide their T-dual interpretation. In Section III we provide the tadpole cancellation conditions in a class of models with arbitrary number of order three Wilson lines. For completeness we also describe the tadpole constraints in the T-dual version, and show (in the Appendix) they are related to the tadpole conditions in the original picture by a discrete Fourier transform. In Section IV we describe in detail the orbifold and orientifold projections, both in terms of D9- and $D5_3$-branes [3], and in a T-dual picture of D3 and $D7_3$-branes, to obtain the spectra of the models in subsequent sections. In Section V we systematically explore the gauge group structure of models with discrete Wilson lines (Subsection V A), and focus on a particular solution (Subsection V B) with potentially phenomenologically interesting features. We also present a solution with anti-branes (Subsection V C), which provides a realistic gauge group with three families. In Section VI we summarize and discuss the results and techniques developed in this paper, and conclude with possible further applications.

II. WILSON LINES IN THE Z_6 ORIENTIFOLD

The techniques to construct $N = 1$ Type IIB orientifolds based on orbifolds $T^6/\mathbf{Z_N}$ and $T^6/(\mathbf{Z_N} \times \mathbf{Z_M})$ are by now standard and we refer the reader to, e.g., [6] for a detailed discussion of such models as well as the notations and conventions.

We shall focus on the study of Wilson lines for $\mathbf{Z_6}$ orientifold, constructed [4,6] by orientifolding type IIB string theory on $T^6/\mathbf{Z_6}$. The $\mathbf{Z_6}$ symmetry is generated by an action θ:

$$\theta : X_i \to e^{2i\pi v_i} X_i \,, \tag{1}$$

on the complex coordinates X_i, $i = 1, 2, 3$ of the three two-tori and the twist vector v is of the form $v = \frac{1}{6}(1, 1, -2)$. The orientifolding is generated by the world-sheet parity operator Ω. The model contains a set of D9- and $D5_3$-branes. The action of θ and Ω on the open string states is described by Chan-Paton matrices γ_θ and γ_Ω, respectively, which

[3] Throughout this paper, we denote by $D5_i$-branes ($D7_i$-branes) the D5-branes (D7-branes) wrapped on (transverse to) the i^{th} complex plane.

form a projective representation of the orientifold group. Hence, consistency with the group multiplication rules implies algebraic constraints like $\gamma_\theta^N = \pm 1$, ($N = 6$ for $\mathbf{Z_6}$ orientifold), $(\gamma_\theta^k)^* = \pm\gamma_\Omega^*\gamma_\theta^k\gamma_\Omega$, etc. In addition, γ_Ω must be symmetric for D9-branes and antisymmetric for D5-branes. In addition, Ramond-Ramond (RR) sector tadpole cancellation conditions must be imposed on the Chan-Paton matrices to ensure the consistency of the theory. After successful embedding of the orientifold action, the open string states, including gauge bosons and matter fields, can be easily constructed.

We shall start with the analysis for the $\mathbf{Z_6}$ orbifold, and only at a later stage incorporate the orientifold projection Ω. Also in this section we shall focus primarily on the algebraic constraints on the model, i.e. we discuss the building blocks for the Wilson lines, leaving the study of tadpole cancellation conditions for the subsequent Sections [4].

The action of θ on D9-branes, $\gamma_{\theta,9}$, has the general form

$$\gamma_{\theta,9} = \mathrm{diag}\,(e^{\pi i\frac{1}{6}}\mathbf{1}_{N_1}, e^{\pi i\frac{3}{6}}\mathbf{1}_{N_2}, e^{\pi i\frac{5}{6}}\mathbf{1}_{N_3}, e^{\pi i\frac{7}{6}}\mathbf{1}_{N_4}, e^{\pi i\frac{9}{6}}\mathbf{1}_{N_5}, e^{\pi i\frac{11}{6}}\mathbf{1}_{N_6})\,. \tag{2}$$

For the time being the non-negative integers N_i are kept arbitrary, but will be eventually constrained by the orientifold projection and tadpole cancellation conditions.

In the following we shall construct different types of discrete Wilson lines on the D9-branes. Since the third complex plane is twisted only by order three actions, the corresponding Wilson lines are identical to those in the $\mathbf{Z_3}$ orientifold [5,6,17]. Hence we focus on Wilson lines along the first complex plane (the second plane suffers identical twists). The (space) group law implies the following set of algebraic constraints on the Chan-Paton embedding $\gamma_{W,9}$ such Wilson lines:

$$\begin{aligned}(\gamma_{\theta,9}\gamma_{W,9})^6 &= -\mathbf{1}\,;\\ (\gamma_{\theta^2,9}\gamma_{W,9})^3 &= -\mathbf{1}\,;\\ (\gamma_{\theta^3,9}\gamma_{W,9})^2 &= -\mathbf{1}\,.\end{aligned} \tag{3}$$

In the following subsections we construct several solutions to these constraint, including order three Wilson lines, order two Wilson lines, and continuous Wilson lines.

---

[4] This approach has an additional advantage that the results in this Section apply to more general sets of branes, e.g., D2-branes wrapped on a complex plane, which could be of interest to study the spectrum of states in such models.

A. Order Three Wilson lines

An order three Wilson line $\gamma_{W_1,9}$ is characterized by the additional condition

$$[\gamma_{\theta^2,9}, \gamma_{W_1,9}] = 0\,, \tag{4}$$

hence the second constraint in (3) implies $\gamma^3_{W_1,9} = \mathbf{1}$. Given the relation between Wilson line eigenvalues and brane locations in a T-dual picture, in the model obtained by T-dualizing along the first complex plane, the configuration corresponds to locating the D7-branes at different fixed points of the order three action θ^2.

In the following we construct a family of Wilson lines satisfying these constraints. It is convenient to reorder the blocks in $\gamma_{\theta,9}$, so that we have

$$\begin{aligned}
\gamma_{\theta,9} &= \mathrm{diag}\,(e^{\pi i\frac{1}{6}}\mathbf{1}_{N_1}, e^{\pi i\frac{7}{6}}\mathbf{1}_{N_4}, e^{\pi i\frac{3}{6}}\mathbf{1}_{N_2}, e^{\pi i\frac{9}{6}}\mathbf{1}_{N_5}, e^{\pi i\frac{5}{6}}\mathbf{1}_{N_3}, e^{\pi i\frac{11}{6}}\mathbf{1}_{N_6})\,;\\
\gamma_{\theta^2,9} &= \mathrm{diag}\,(e^{\pi i\frac{1}{3}}\mathbf{1}_{N_1}, e^{\pi i\frac{1}{3}}\mathbf{1}_{N_4}, -\mathbf{1}_{N_2}, -\mathbf{1}_{N_5}, e^{\pi i\frac{5}{3}}\mathbf{1}_{N_3}, e^{\pi i\frac{5}{3}}\mathbf{1}_{N_6})\,;\\
\gamma_{\theta^3,9} &= \mathrm{diag}\,(i\mathbf{1}_{N_1}, -i\mathbf{1}_{N_4}, -i\mathbf{1}_{N_2}, i\mathbf{1}_{N_5}, i\mathbf{1}_{N_3}, -i\mathbf{1}_{N_6}).
\end{aligned} \tag{5}$$

The most general form of $\gamma_{W_1,9}$ which satisfies the condition (4) is

$$\gamma_{W_1,9} = \begin{pmatrix} \gamma^A_{W_1,9} & & \\ & \gamma^B_{W_1,9} & \\ & & \gamma^C_{W_1,9} \end{pmatrix}, \tag{6}$$

where each piece in the matrix above spans two blocks in (5). The second constraint in Eqn.(3) becomes $(\gamma^{(p)}_{W_1,9})^3 = \mathbf{1}$, $(p) = A, B, C$. One can show that the third constraint in (3) implies the first, so we need to impose the former only.

The matrices $\gamma^{(p)}_{W_1,9}$, $p = A, B, C$ may contain diagonal blocks of identity matrices with various dimensionalities, which correspond to entries for which the Wilson line has a trivial action. In the following discussion, we will tacitly remove those entries, and define $N_i^{'}$ to number the entries with non-diagonal block structures.

There are non-trivial solutions for the constraints above when the (redefined) $N_i^{'}$ satisfy $N_1^{'} = N_4^{'}$, $N_2^{'} = N_5^{'}$, $N_3^{'} = N_6^{'}$. For instance, let us consider

$$\gamma^A_{W_1,9} = \begin{pmatrix} \frac{1}{2}(A+A^2) & \frac{1}{2}(A-A^2) \\ \frac{1}{2}(A-A^2) & \frac{1}{2}(A+A^2) \end{pmatrix} \quad ; \quad \gamma^B_{W_1,9} = \begin{pmatrix} \frac{1}{2}(B+B^2) & \frac{1}{2}(B-B^2) \\ \frac{1}{2}(B-B^2) & \frac{1}{2}(B+B^2) \end{pmatrix};$$

$$\gamma^C_{W_1,9} = \begin{pmatrix} \frac{1}{2}(C+C^2) & \frac{1}{2}(C-C^2) \\ \frac{1}{2}(C-C^2) & \frac{1}{2}(C+C^2) \end{pmatrix}, \tag{7}$$

where A, B and C are diagonal matrices satisfying $A^3 = \mathbf{1}$, $B^3 = \mathbf{1}$, $C^3 = \mathbf{1}$. A direct calculation, starting from constraints in Eqn.(3) and Eqn.(4), confirms that the building

blocks $\gamma_{W_1,9}^{A,B,C}$ of the the Wilson line (6), are indeed of the form given in Eqn.(7), and therefore define a consistent order three Wilson line for the $\mathbf{Z_6}$ orbifold.

To clarify the structure of our solution, let us diagonalize A, B and C matrices, while maintaining $\gamma_{\theta^2,9}$ diagonal, but making $\gamma_{\theta^3,9}$ non-diagonal. Denoting matrices in the new basis with a tilde, we have

$$\tilde{A} = \mathrm{diag}\,(\mathbf{1}_{n_1}, \alpha\mathbf{1}_{m_1}, \alpha^2\mathbf{1}_{m_1}) \;\; ; \;\; \tilde{B} = \mathrm{diag}\,(\mathbf{1}_{n_2}, \alpha\mathbf{1}_{m_2}, \alpha^2\mathbf{1}_{m_2}) \;\; ; \;\; \tilde{C} = \mathrm{diag}\,(\mathbf{1}_{n_3}, \alpha\mathbf{1}_{m_3}, \alpha^2\mathbf{1}_{m_3})\,, \quad (8)$$

with $\alpha = e^{2\pi i/3}$. Hence we have

$$\tilde{\gamma}_{W_1,9} = \mathrm{diag}\,(\mathbf{1}_{N_1+N_4-2m_1}, \alpha\mathbf{1}_{m_1}, \alpha^2\mathbf{1}_{m_1}, \mathbf{1}_{N_2+N_5-2m_2}, \alpha\mathbf{1}_{m_2}, \alpha^2\mathbf{1}_{m_2}, \mathbf{1}_{N_3+N_6-2m_3}, \alpha\mathbf{1}_{m_3}, \alpha^2\mathbf{1}_{m_3}), \quad (9)$$

where N_i are as originally defined in Eqn.(5), while m_1, m_2 and m_2 are non-negative integers satisfying $N_1 + N_4 - 2m_1 \geq 0$, $N_2 + N_5 - 2m_2 \geq 0$ and $N_3 + N_6 - 2m_3 \geq 0$. On the other hand

$$\tilde{\gamma}_{\theta^3,9} = i\ \mathrm{diag}\,(T_{11}, T_{22}, T_{33}), \quad (10)$$

where the matrix T_{11} is defined as

$$T_{11} = \begin{pmatrix} \mathbf{1}_{N_1-m_1} & & & \\ & -\mathbf{1}_{N_4-m_1} & & \\ & & & \mathbf{1}_{m_1} \\ & & \mathbf{1}_{m_1} & \end{pmatrix}, \quad (11)$$

and T_{22} and T_{33} are defined analogously.

In this basis the structure of the Wilson line nicely reflects the configuration of D7-branes in the T-dual picture. Each eigenspace of $\tilde{\gamma}_{W_1,9}$ corresponds to a set of D7-branes at a θ^2 fixed points. The action of $\tilde{\gamma}_{\theta^3}$ leaves invariant the eigenspace with $\tilde{\gamma}_{W_1}$-eigenvalue 1, and swaps the eigenspaces of $\tilde{\gamma}_{W_1}$-eigenvalues α, α^2. In the T-dual picture, this corresponds to the fact that θ^3 action leaves D7-branes at the origin fixed, but it exchanges D7-branes at the remaining two θ^2 fixed points.

We conclude this subsection by studying the introduction of a second discrete order three Wilson line $\gamma_{W_2,9}$ in the second complex plane. This Wilson line has to satisfy all the conditions in Eqs.(3) and Eqn.(4), and in addition has to commute with the first Wilson line action, i.e. $[\gamma_{W_2,9}, \gamma_{W_1,9}] = 0$. In the basis in which $\gamma_{W_1,9}$ is diagonal these constraints can be easily satisfied by the following form of $\gamma_{W_2,9}$ (for the sake of simplicity we have omitted the notation with a tilde):

$$\gamma_{W_2,9} = \mathrm{diag}\,(Q_{11}, Q_{22}, Q_{33}), \tag{12}$$

where the matrix Q_{11} is defined as

$$Q_{11} = \mathrm{diag}\,(q_{11}, q_{12}, q_{13}), \tag{13}$$

the matrices q_{1i} $(i = 1, 2, 3)$ are defined as

$$q_{11} = \begin{pmatrix} \mathbf{1}_{N_1+N_4-2m_1-2x_1} & & \\ & \frac{1}{2}(D+D^2) & \frac{1}{2}(D-D^2) \\ & \frac{1}{2}(D-D^2) & \frac{1}{2}(D+D^2) \end{pmatrix}; \tag{14}$$

$$q_{12} = \mathrm{diag}\,(\mathbf{1}_{m_1-x_2-x_3}, \alpha\mathbf{1}_{x_2}, \alpha^2\mathbf{1}_{x_3}) \quad ; \quad q_{13} = \mathrm{diag}\,(\mathbf{1}_{m_1-x_2-x_3}, \alpha^2\mathbf{1}_{x_2}, \alpha\mathbf{1}_{x_3}), \tag{15}$$

where $D^3 = 1$ and D is a matrix of dimension $x_1 \times x_1$, while $x_2 + x_3 \leq m_1$. Matrices Q_{22} and Q_{33} can be defined analogously with a set of integer parameters x_i $(i = 1, \ldots, 12)$.

B. Order two Wilson lines

We now turn to the generic structure of order two Wilson lines. An order two Wilson line in the first complex plane acts on the D9-branes with Chan-Paton matrix $\gamma_{W2_1,9}$. This embedding must satisfy the set of algebraic constraints in Eqn.(3). In addition, it must satisfy the commutation relation

$$[\gamma_{\theta,9}, \gamma_{W2_1,9}] = 0\ . \tag{16}$$

Thus, the third constraint in (3) becomes $\gamma^2_{W2_1,9} = \mathbf{1}$. These Wilson lines correspond in a T-dual picture to branes sitting at the θ^3 fixed points.

It is convenient to reorder the Chan-Paton blocks as follows

$$\begin{aligned} \gamma_{\theta,9} &= \mathrm{diag}\,(e^{\pi i\frac{9}{6}}\mathbf{1}_{N_5}, e^{\pi i\frac{1}{6}}\mathbf{1}_{N_1}, e^{\pi i\frac{5}{6}}\mathbf{1}_{N_3}, e^{\pi i\frac{3}{6}}\mathbf{1}_{N_2}, e^{\pi i\frac{11}{6}}\mathbf{1}_{N_6}, e^{\pi i\frac{7}{6}}\mathbf{1}_{N_4})\ ; \\ \gamma_{\theta^2,9} &= \mathrm{diag}\,(e^{\pi i}\mathbf{1}_{N_5}, e^{\pi i\frac{1}{3}}\mathbf{1}_{N_1}, e^{\pi i\frac{5}{3}}\mathbf{1}_{N_3}, e^{\pi i}\mathbf{1}_{N_2}, e^{\pi i\frac{5}{3}}\mathbf{1}_{N_6}, e^{\pi i\frac{1}{3}}\mathbf{1}_{N_4})\ ; \\ \gamma_{\theta^3,9} &= \mathrm{diag}\,(i\mathbf{1}_{N_5}, i\mathbf{1}_{N_1}, i\mathbf{1}_{N_3}, -i\mathbf{1}_{N_2}, -i\mathbf{1}_{N_6}, -i\mathbf{1}_{N_4})\ . \end{aligned} \tag{17}$$

The general form of a Wilson line matrix, satisfying Eqn.(16), is of the form

$$\gamma_{W2_1,9} = \begin{pmatrix} \gamma^A_{W2_1,9} & \\ & \gamma^B_{W2_1,9} \end{pmatrix}, \tag{18}$$

where each piece in the above matrix spans three blocks in (17). The third constraint in (3) becomes $(\gamma^{(p)}_{W2_1,9})^2 = \mathbf{1}$, for $(p) = A, B$.

The constraints can be solved independently for the two building blocks $\gamma^A_{W2_1}$ and $\gamma^B_{W2_1}$. Since they are analogous, we detail only the 'A' block. Let us denote $\gamma^A_{\theta^k,9}$, the relevant sub-block in the $\mathbf{Z_6}$ Chan-Paton embeddings.

The matrices $\gamma^{(p)}_{W2_1,9}$, $p = A, B$ may contain diagonal pieces. They would correspond to entries for which the Wilson line has a trivial action. We again redefine the N_i to number the entries with non-diagonal block structures.

There are non-trivial solutions for the constraints above when the (redefined) N_i's satisfy $N_1 = N_3 = N_5$, $N_2 = N_4 = N_6$. In analogy with the order three Wilson lines, it is convenient to go to the basis in which $\gamma_{W2_1,9}$ and $\gamma_{\theta^3,9}$ are simultaneously diagonalized, while other matrices like $\gamma_{\theta,9}$ become off-diagonal. We denote the matrices in this new basis by a tilde. The structure of $\tilde{\gamma}^A_{W2_1,9}$ and $\tilde{\gamma}^A_{\theta^3,9}$ is

$$\begin{aligned} \tilde{\gamma}^A_{\theta^3,9} &= \mathrm{diag}\,(i\mathbf{1}, i\mathbf{1}, i\mathbf{1})\ ; \\ \tilde{\gamma}^A_{W_1,9} &= \mathrm{diag}\,(A_1, A_2, A_3)\ , \end{aligned} \tag{19}$$

where A_1, A_2, A_3 are diagonal and square to $\mathbf{1}$.

In this basis the (non-diagonal) matrix $\tilde{\gamma}^A_{\theta^2,9}$ has the structure

$$\tilde{\gamma}^A_{\theta^2,9} = -\begin{pmatrix} & \mathbf{1} & \\ & & \mathbf{1} \\ \mathbf{1} & & \end{pmatrix}\ . \tag{20}$$

In order to impose the second constraint in (3), we obtain

$$(\tilde{\gamma}^A_{\theta^2,9}\tilde{\gamma}^A_{W_1,9})^3 = -\begin{pmatrix} A_2A_3A_1 & & \\ & A_3A_1A_2 & \\ & & A_1A_2A_3 \end{pmatrix}\ . \tag{21}$$

Thus, we get the constraint $A_1A_2A_3 = \mathbf{1}$ (since the matrices A_i are diagonal and hence commute, one automatically obtains that $A_2A_3A_1 = \mathbf{1}$ and $A_3A_1A_2 = \mathbf{1}$ as well.).

The matrix $\tilde{\gamma}^A_{\theta,9}$ can be obtained as $-\tilde{\gamma}^A_{\theta^3,9}(\tilde{\gamma}^A_{\theta^2,9})^2$, hence the first constraint in (3) is automatically satisfied.

In order to express these matrices in the original basis, where all the $\gamma_{\theta^k,9}$ are diagonal, and $\gamma_{W2_1,9}$ is non-diagonal, we change the basis using the unitary transformation

$$P = \frac{1}{\sqrt{3}}\begin{pmatrix} 1 & 1 & 1 \\ 1 & \alpha & \alpha^2 \\ 1 & \alpha^2 & \alpha \end{pmatrix}\ . \tag{22}$$

We get

$$P\tilde{\gamma}^A_{\theta^2,9}P^{-1} = -\mathrm{diag}\,(\mathbf{1}, \alpha^2\mathbf{1}, \alpha\mathbf{1})\ , \tag{23}$$

which is precisely the form for $\gamma_{\theta^2,9}$ in the initial basis. In the initial basis the Wilson line has the following structure

$$\gamma^A_{W2_1,9} = P\tilde{\gamma}^A_{W2_1,9}P^{-1} = \begin{pmatrix} A & A^{\alpha^2} & A^{\alpha} \\ A^{\alpha} & A & A^{\alpha^2} \\ A^{\alpha^2} & A^{\alpha} & A \end{pmatrix}\ , \tag{24}$$

where we have defined

$$A = \frac{1}{3}(A_1 + A_2 + A_3) \quad ; \quad A^{\alpha} = \frac{1}{3}(A_1 + \alpha A_2 + \alpha^2 A_3) \quad ; \quad A^{\alpha^2} = \frac{1}{3}(A_1 + \alpha^2 A_2 + \alpha A_3)\ . \tag{25}$$

Naturally, this Wilson line satisfies all the algebraic constraints (3).

The structure of these Wilson lines (particularly in the rotated basis, where these Wilson lines are diagonal) reflects the distribution of D7-branes in the T-dual picture. Since the Wilson line commutes with the θ^3 twist, in the T-dual picture D7-branes are at θ^3 fixed points. The order three permutation action (20) corresponds, in the T-dual picture, to the permutation action of θ^2 on the three θ^3 fixed points away from the origin.

C. Continuous Wilson line in a $\mathbf{Z_6}$ plane

In this section we compute the structure of a continuous Wilson line embedded along the first plane, $\gamma_{Wc,9}$. It is convenient to reorder the blocks in the Chan-Paton matrices as

$$\begin{aligned}
\gamma_{\theta,9} &= \mathrm{diag}\,(e^{\pi i\frac{1}{6}}\mathbf{1}_{N_1}, e^{\pi i\frac{9}{6}}\mathbf{1}_{N_5}, e^{\pi i\frac{5}{6}}\mathbf{1}_{N_3}, e^{\pi i\frac{7}{6}}\mathbf{1}_{N_4}, e^{\pi i\frac{3}{6}}\mathbf{1}_{N_2}, e^{\pi i\frac{11}{6}}\mathbf{1}_{N_6})\ ; \\
\gamma_{\theta^2,9} &= -\mathrm{diag}\,(e^{2\pi i\frac{2}{3}}\mathbf{1}_{N_1}, \mathbf{1}_{N_5}, e^{2\pi i\frac{1}{3}}\mathbf{1}_{N_3}, e^{2\pi i\frac{2}{3}}\mathbf{1}_{N_4}, \mathbf{1}_{N_2}, e^{2\pi i\frac{1}{3}}\mathbf{1}_{N_6})\ ; \\
\gamma_{\theta^3,9} &= \mathrm{diag}\,(i\mathbf{1}_{N_1}, i\mathbf{1}_{N_5}, i\mathbf{1}_{N_3}, -i\mathbf{1}_{N_4}, -i\mathbf{1}_{N_2}, -i\mathbf{1}_{N_6})\ .
\end{aligned} \tag{26}$$

The continuous Wilson line will involve an equal number of entries from each diagonal block (i.e. a combination of D-branes with the traceless embedding). Therefore, in the following discussion of the continuous Wilson line we take all the N_i's to be equal.

Since the structure of continuous Wilson lines, consistent with an order three orbifold twist, is known [5,6,17], it is convenient to use this information to solve the second constraint in (3). One then imposes the additional conditions to obtain the final form of the Wilson line in the $\mathbf{Z_6}$ case.

The order three twist can be written in the following form:

$$\gamma_{\theta^2} = -\mathrm{diag}\,(e^{2\pi i\frac{2}{3}}, 1, e^{2\pi i\frac{1}{3}}, e^{2\pi i\frac{2}{3}}, 1, e^{2\pi i\frac{1}{3}}) \otimes \mathbf{1}_N \ . \tag{27}$$

The structure of a continuous Wilson line consistent with the order three twist is

$$\tilde{\gamma}_{W,9} = \mathrm{diag}\,(\gamma_{c,1}; \gamma_{c,2}) \otimes \mathbf{1}_N \ , \tag{28}$$

where $\gamma_{c,1}$, $\gamma_{c,2}$ are two independent 3×3 matrices, each of which depends on one complex parameter. They must satisfy $(\gamma_{c,i}\gamma_{Z_3})^3 = \mathbf{1}$, where $\gamma_{Z_3} = \mathrm{diag}\,(1, e^{2\pi i\frac{1}{3}}, e^{2\pi i\frac{2}{3}})$, and are of the general form, parameterized by one complex parameter, as given in [17]. (The one real parameter continuous $\mathbf{Z_3}$ Wilson line was first given in [5,6].) We have introduced a tilde notation in the Wilson line above because it has such a simple form only in a rotated basis, where the matrices γ_θ, γ_{θ^3} become non-diagonal. Specifically, the θ^3 twist is embedded as

$$\tilde{\gamma}_{\theta^3,9} = i \begin{pmatrix} & \mathbf{1}_3 \\ \mathbf{1}_3 & \end{pmatrix} \otimes \mathbf{1}_N. \tag{29}$$

Hence, the second condition in (3) requires $\gamma_{c,2} = \gamma_{c,1}^{-1}$. From now on we denote $\gamma_{c,1}$, $\gamma_{c,2}$ simply by γ, γ^{-1}, and also define $\gamma_+ \equiv \frac{1}{2}(\gamma + \gamma^{-1})$, $\gamma_- \equiv \frac{1}{2}(\gamma - \gamma^{-1})$.

Rotating back to the original basis, we have

$$\begin{aligned}
\gamma_{\theta,9} &= \mathrm{diag}\,(e^{\pi i\frac{1}{6}}, e^{\pi i\frac{9}{6}}, e^{\pi i\frac{5}{6}}, e^{\pi i\frac{7}{6}}, e^{\pi i\frac{3}{6}}, e^{\pi i\frac{11}{6}}) \ ; \\
\gamma_{\theta^2,9} &= -\mathrm{diag}\,(e^{2\pi i\frac{2}{3}}, 1, e^{2\pi i\frac{1}{3}}, e^{2\pi i\frac{2}{3}}, 1, e^{2\pi i\frac{1}{3}}) \ ; \\
\gamma_{\theta^3,9} &= \mathrm{diag}\,(i, i, i, -i, -i, -i) \ ; \\
\gamma_{W,9} &= \begin{pmatrix} \gamma_+ & \gamma_- \\ \gamma_- & \gamma_+ \end{pmatrix} \ ,
\end{aligned} \tag{30}$$

in which only one diagonal block of the γ_{θ^k} matrices is shown. The matrix $\gamma_{W,9}$ provides a one (complex) parameter Wilson line solving the second and third constraints. A lengthy, but straightforward calculation shows that it also satisfies the first constraint. Hence, the matrix above provides a continuous Wilson line consistent with all algebraic constraints. The Ansatz (28) can be extended to a more general form, depending on N complex parameters, as

$$\tilde{\gamma}_{W,9} = \bigoplus_{i=1}^{N} \mathrm{diag}\,(\gamma_{c_i}; \gamma_{c_i}^{-1}) \,, \tag{31}$$

with γ_{c_i} a matrix of the form determined in [17], and depending on the i^{th} complex parameter.

The construction above has a clear interpretation in the T-dual picture. A continuous Wilson line corresponds to placing a dynamical D-brane at a generic point on the orbifold. Equivalently, such a D-brane corresponds to a $\mathbf{Z_6}$-invariant set of six D-branes in the covering space. Imposing the order three constraint on the Wilson line amounts to grouping the T-dual D-branes in two $\mathbf{Z_3}$-invariant sets. The additional order two condition relates the locations of the two trios, yielding a $\mathbf{Z_6}$-invariant configuration.

At particular points in the moduli space of continuous Wilson lines, the matrix $\gamma_{Wc,9}$ reproduces the structures encountered in the construction of order three and order two discrete Wilson lines. When the relation $[\gamma_{\theta^2}, \gamma_{W,9}] = 0$ is imposed, one recovers the order three discrete Wilson line: the matrix γ can be diagonalized simultaneously with γ_{θ^2}, hence it reduces to the previous order three discrete Wilson line. In the case of order two discrete Wilson lines, the relation $[\gamma_{\theta^3}, \gamma_{W,9}] = 0$ requires $\gamma = \gamma^{-1}$. The explicit form for the one complex parameter continuous Wilson line γ, as given in [17], allows one to reduce γ precisely to the form of the order two discrete Wilson line solution, given in Eqn.(24), up to an irrelevant overall phase.

In the T-dual picture, these special points in moduli space correspond to configurations where the branes are located at fixed points of θ^2 or θ^3, as explained in the previous two Subsections.

III. TADPOLE CANCELLATION CONDITIONS

Consistent orientifold constructions also requires the conditions of cancellation of RR tadpoles. These have been computed for the $\mathbf{Z_6}$ orientifold in [4,6] for the case without Wilson lines, and require the introduction of D9- and $D5_3$-branes with constrained Chan-Paton embeddings. Tadpole conditions can be easily modified to include the possibility of Wilson lines. Crosscap contributions (twisted orientifold charges) are unchanged, since the closed string sector does not feel the Wilson lines. Disk contributions to twisted tadpoles at a fixed point are proportional to the trace of the D-brane Chan-Paton embedding felt *locally* at the fixed point, which depends on the presence of the Wilson lines.

Using the results in [4,6] and the above properties of the one-loop diagrams in the presence of Wilson lines, it is straightforward to write the tadpole cancellation conditions for general configurations in the presence of Wilson lines. For instance, we consider configurations containing D9-branes, with Wilson lines along all three complex planes, and $D5_3$-branes, with Wilson lines along the third plane, and located at all possible θ^2 fixed points in the

first two planes (labelled by (m,n), with $m,n=0,\pm1$ for shorthand). The twisted tadpole conditions for the different fixed points are:

Fixed point	Twisted Tadpole Condition
$(0,0,p)$	$\mathrm{Tr}\,(\gamma_{\theta,9}\gamma^{p}_{W_3,9}) + \mathrm{Tr}\,(\gamma_{\theta,5_3,(0,0)}\gamma^{p}_{W_3,5_3,(0,0)}) = 0$;
	$\mathrm{Tr}\,(\gamma_{\theta^2,9}\gamma^{2p}_{W_3,9}) + 3\mathrm{Tr}\,(\gamma_{\theta^2,5_3,(0,0)}\gamma^{2p}_{W_3,5_3,(0,0)}) = 16$;
	$\mathrm{Tr}\,(\gamma_{\theta^3,9}) + 4\mathrm{Tr}\,(\gamma_{\theta^3,5_3,(0,0)}) = 0$;
	$\mathrm{Tr}\,(\gamma_{\theta^4,9}\gamma^{p}_{W_3,9}) + 3\mathrm{Tr}\,(\gamma_{\theta^4,5_3,(0,0)}\gamma^{p}_{W_3,5_3,(0,0)}) = -16$;
	$\mathrm{Tr}\,(\gamma_{\theta^5,9}\gamma^{2p}_{W_3,9}) + \mathrm{Tr}\,(\gamma_{\theta^5,5_3,(0,0)}\gamma^{2p}_{W_3,5_3,(0,0)}) = 0$;
(m,n,p)	$\mathrm{Tr}\,(\gamma_{\theta^2,9}\gamma^{m}_{W_1,9}\gamma^{n}_{W_2,9}\gamma^{2p}_{W_3,9}) + 3\mathrm{Tr}\,(\gamma_{\theta^2,5_3,(m,n)}\gamma^{2p}_{W_3,5_3,(m,n)}) = 4$;
$(m,n)\neq(0,0)$	$\mathrm{Tr}\,(\gamma_{\theta^4,9}\gamma^{2m}_{W_1,9}\gamma^{2n}_{W_2,9}\gamma^{p}_{W_3,9}) + 3\mathrm{Tr}\,(\gamma_{\theta^4,5_3,(m,n)}\gamma^{p}_{W_3,5_3,(m,n)}) = -4$. (32)

In subsequent sections we will provide a systematic search for solutions to these conditions. In fact, it will be practical to consider the models obtained after T-dualizing along the third complex plane, so that Wilson lines along it become D-brane positions in the T-dual picture. The original D9-branes become D7_3-branes, sitting at the three θ^2 fixed points in the third plane, labelled by $p=0,\pm1$, and the D5_3-branes become D3-branes, sitting at θ^2 fixed points (m,n,p). The orientifold action in the T-dual version is $\Omega_3=\Omega R_3(-)^{F_L}$, with $R_3: z_3\to -z_3$.

In order to construct the model in the T-dual version, we need to derive the corresponding tadpole cancellation conditions. These can be obtained from the original ones, given in Eqn.(32), by applying the Fourier transformation procedure, discussed in the Appendix. Applying this procedure along the third complex plane, the new tadpole conditions read:

Fixed point	Twisted Tadpole Condition
$(0,0,p)$	$\mathrm{Tr}\,(\gamma_{\theta,7_3,p}) + \mathrm{Tr}\,(\gamma_{\theta,3,(0,0,p)}) = 0$;
	$\mathrm{Tr}\,(\gamma_{\theta^2,7_3,p}) + 3\mathrm{Tr}\,(\gamma_{\theta^2,3,(0,0,p)}) = 16\delta_{p,0}$;
	$\sum_{p=0,\pm1}\left[\,\mathrm{Tr}\,(\gamma_{\theta^3,7_3,p}) + 4\mathrm{Tr}\,(\gamma_{\theta^3,3,(0,0,p)})\,\right] = 0$;
	$\mathrm{Tr}\,(\gamma_{\theta^4,7_3,p}) + 3\mathrm{Tr}\,(\gamma_{\theta^4,3,(0,0,p)}) = -16\delta_{p,0}$;
	$\mathrm{Tr}\,(\gamma_{\theta^5,7_3,p}) + \mathrm{Tr}\,(\gamma_{\theta^5,3,(0,0,p)}) = 0$;
(m,n,p)	$\mathrm{Tr}\,(\gamma_{\theta^2,7_3,p}\gamma^{m}_{W_1,7_3,p}\gamma^{n}_{W_2,7_3,p}) + 3\mathrm{Tr}\,\gamma_{\theta^2,3,(m,n,p)} = 4\delta_{p,0}$;
$(m,n)\neq(0,0)$	$\mathrm{Tr}\,(\gamma_{\theta^4,7_3,p}\gamma^{2m}_{W_1,7_3,p}\gamma^{2n}_{W_2,7_3,p}) + 3\mathrm{Tr}\,\gamma_{\theta^2,3,(m,n,p)} = -4\delta_{p,0}$. (33)

These conditions nicely reflect the geometric structure of the fixed points in the T-dual picture, which is depicted in Fig. 1. It represents the 27 θ^2 fixed points of $T^6/\mathbf{Z_6}$, each with its contribution to the θ^2-twisted crosscap tadpole which, if non-zero, has to be canceled by D3 branes sitting at (or D7_3-branes passing through) those points. Notice that crosscap tadpoles arise only at fixed points of Ω_3, which therefore must have $p = 0$. Recall also that θ^3 reflects z_1 and z_2, so only points with $m = n = 0$ are fixed under it. Taking all these conditions into account, we see the following properties of the tadpole cancellation conditions:

- The point $(0, 0, 0)$ is fixed under θ^2, θ^3 and Ω_3, it is a $\mathbf{C^3/Z_6}$ orientifold point. The contributions to the θ^k crosscap tadpoles for such point can be computed to be 0, 16, 0, -16, 0 for $k = 1, ..., 5$, as above.

- A point of the form $(m, n, 0)$ with $(m, n) \neq (0, 0)$ is fixed under θ^2 and Ω_3, but not under θ^2, and so is a $\mathbf{C^3/Z_3}$ orientifold point. The crosscap tadpoles in its two twisted sectors are 4, -4 [20], as above.

- Points of the form $(0, 0, p)$ for non-zero p, are fixed under θ^2, θ^3, but not under Ω_3; they are $\mathbf{C^3/Z_6}$ orbifold points, and have zero crosscap tadpoles.

- Points of the form (m, n, p) for non-zero p and $(m, n) \neq (0, 0)$ are fixed under θ^2 but not under θ^3 or Ω_3; they are $\mathbf{C^3/Z_3}$ orbifold points, and do not receive crosscap tadpoles.

As discussed in [18], $\mathbf{C^3/Z_3}$ orbifold points are interesting to build three-family models with realistic gauge groups on the D3-branes. The $\mathbf{Z_3}$ symmetry ensures three families structure, while the orbifold (rather than orientifold) points ensures the existence of one non-anomalous U(1) which could play the role of hypercharge, if the gauge groups arising from these D3-branes contain $SU(3)_{color} \times SU(2)_L \times U(1)$. The existence of $\mathbf{Z_3}$ orbifold points is one of the motivations for studying $\mathbf{Z_6}$ orientifold.

IV. SPECTRUM

Before turning to the techniques of solving the tadpole conditions and exploring their solutions, we devote this section to deriving the spectrum in the open string sectors by imposing orbifold and orientifold projections.

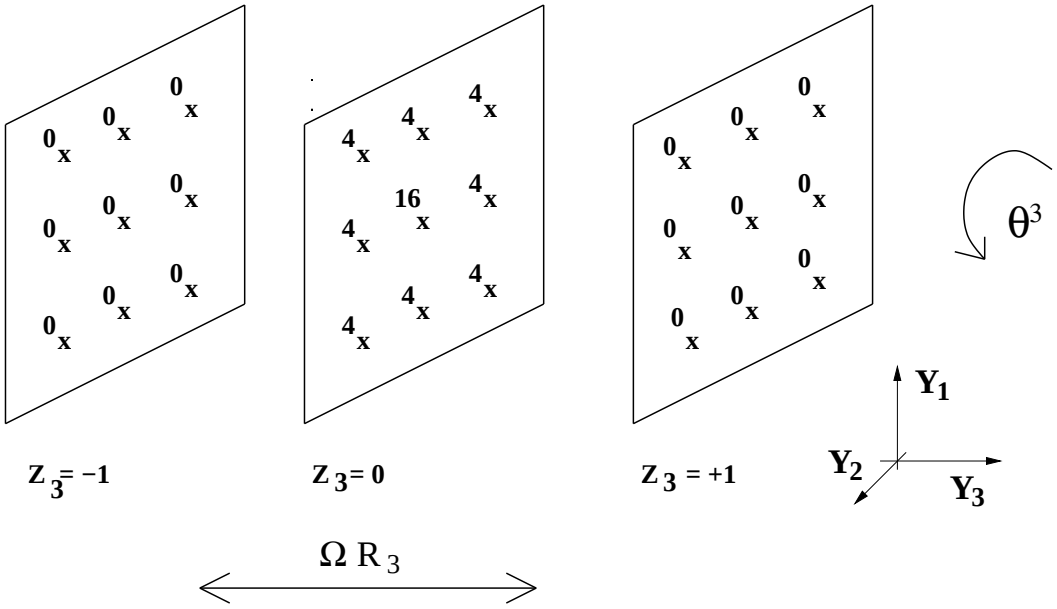

FIG. 1. Structure of $T^6/\mathbf{Z_6}$ modded out by Ω_3. At each θ^2 fixed point we have indicated the θ^2-twisted crosscap tadpole. This has to be canceled by including D3-branes (denoted by crosses) and D7$_3$-branes (depicted as planes) sitting or passing through those points.

The class of models we are considering, as mentioned above, includes models with D9-branes with arbitrary order three Wilson lines along the three complex planes, and D5$_3$-branes at the diverse θ^2 fixed points in the first two complex planes, and with an arbitrary order three Wilson line on the third plane.

In the 99 sector the projections for gauge bosons and chiral multiplets are

$$\begin{array}{lll} \mathbf{99} & \text{Gauge} & \lambda = \gamma_{\theta,9}\lambda\gamma^{-1}_{\theta,9}\ ; \quad \lambda = -\gamma_{\Omega,9}\lambda^T\gamma^{-1}_{\Omega,9}\ ; \\ & i^{th}\text{Chiral} & \lambda = e^{2\pi i v_i}\gamma_{\theta,9}\lambda\gamma^{-1}_{\theta,9}\ ; \quad \lambda = -\gamma_{\Omega,9}\lambda^T\gamma^{-1}_{\Omega,9}\ , \end{array} \tag{34}$$

where $i = 1, 2, 3$ labels the complex planes. Also, since boundary conditions allow for momentum excitations in all complex planes, we have to impose the projection onto states invariant under the action of the three Wilson lines

$$\mathbf{99}\quad \lambda = \gamma_{W_i,9}\lambda\gamma^{-1}_{W_i,9}\ \text{ for all 99 states}\ , \tag{35}$$

for $i = 1, 2, 3$. In the $5_3 5_3$ sector, we obtain states only for open strings stretching between the D5$_3$-branes sitting at identical points (m, n) in the first two planes. The projections for gauge bosons and chiral multiplets are

$$\begin{array}{lll} \mathbf{5_3 5_3} & \text{Gauge} & \lambda = \gamma_{\theta,5_3,(m,n)}\lambda\gamma^{-1}_{\theta,5_3,(m,n)}\ ; \quad \lambda = -\gamma_{\Omega,5_3,(m,n)}\lambda^T\gamma^{-1}_{\Omega,5_3,(m,n)}\ ; \\ & \text{Chiral} & \lambda = e^{2\pi i v_i}\gamma_{\theta,5_3,(m,n)}\lambda\gamma^{-1}_{\theta,5_3,(m,n)}\ ;\ \lambda = \pm\gamma_{\Omega,5_3,(m,n)}\lambda^T\gamma^{-1}_{\Omega,5_3,(m,n)}\ , \end{array} \tag{36}$$

with $i = 1, 2, 3$, and with the sign in the last equation positive for $i = 1, 2$, and negative for $i = 3$. Since boundary conditions allow for momentum excitations in the third complex planes, all states must satisfy

$$\mathbf{5_3 5_3} \quad \lambda = \gamma_{W_3,5_3,(m,n)} \lambda \gamma^{-1}_{W_3,5_3,(m,n)} \quad \text{for all } 5_3 5_3 \text{ states} . \tag{37}$$

Finally, we turn to the 95_3 sector. There is one such sector for each point (m, n) at which D5_3-branes sit. Since Ω maps it to the $5_3 9$ sector, we keep only the former and do not impose any Ω projection. In performing the orbifold projection one should realize that at a point with coordinates (m, n) in the first two planes the θ action felt by the D9-branes depends on the Wilson lines along these directions. We have the projection

$$\mathbf{95_3} \quad \lambda = e^{-\pi i v_3} (\gamma_{\theta,9} \gamma^m_{W_1,9} \gamma^n_{W_2,9}) \lambda \gamma^{-1}_{\theta,5_3,(m,n)} . \tag{38}$$

In addition since boundary conditions allow for momentum along the third plane, we have to impose

$$\mathbf{95_3} \quad \lambda = \gamma_{W_3,9} \lambda \gamma^{-1}_{W_3,5_3,(m,n)} \quad \text{for } 95_3 \text{ states} . \tag{39}$$

In the T-dual version, in which the orientifold action is Ω_3, and the model contains D7_3- and D3-branes, it is convenient to describe the projections in these terms as well. Our class of models contains D7_3-branes sitting at θ^2 fixed points in the third plane, and with arbitrary order three Wilson lines along the first two, and D3-branes sitting at θ^2 fixed points (m, n, p) in the internal space.

In the $7_3 7_3$ sector there are massless states only when both 7_3 branes sit at the same location in the third plane (this is T-dual to the W_3 projection in (35)). The only D7_3-branes that are left fixed by Ω_3 projection sit at $p = 0$. For these, the projections read

$$\begin{array}{lll} \mathbf{7_3 7_3} & \text{Gauge} & \lambda = \gamma_{\theta,7_3,0} \lambda \gamma^{-1}_{\theta,7_3,0} \; ; \quad \lambda = -\gamma_{\Omega_3,7_3,0} \lambda^T \gamma^{-1}_{\Omega_3,7_3,0} \; ; \\ & i^{th}\text{Chiral} & \lambda = e^{2\pi i v_i} \gamma_{\theta,7_3,0} \lambda \gamma^{-1}_{\theta,7_3,0} \; ; \quad \lambda = -\gamma_{\Omega_3,7_3,0} \lambda^T \gamma^{-1}_{\Omega_3,7_3,0} . \end{array} \tag{40}$$

For D7_3-branes at a location $p \neq 0$, Ω_3 maps them to D7_3-branes at the location $-p$. Hence, we may keep only one set of them, say $p = +1$, and do not impose the orientifold projection. We have

$$\begin{array}{lll} \mathbf{7_3 7_3} & \text{Gauge} & \lambda = \gamma_{\theta,7_3,+1} \lambda \gamma^{-1}_{\theta,7_3,+1} \; ; \\ & i^{th}\text{Chiral} & \lambda = e^{2\pi i v_i} \gamma_{\theta,7_3,+1} \lambda \gamma^{-1}_{\theta,7_3,+1} . \end{array} \tag{41}$$

Since boundary conditions allow for momentum excitations in the first two complex planes, we have the Wilson line projection

$$\mathbf{7_3 7_3} \quad \lambda = \gamma_{W_i,7_3,p} \lambda \gamma^{-1}_{W_i,7_3,p} \quad \text{for all } 7_3 7_3 \text{ states} \tag{42}$$

for $p = 0, \pm 1$ and $i = 1, 2$.

In the 33 sector, we obtain states only for D3-branes sitting at the identical points (m, n, p). Notice that all D3-branes sit at θ^2 fixed points, hence all 33 states are subject to the θ^2 projection. However, D3-branes with $(m, n) \neq (0, 0)$ are not fixed under θ, which maps them to D3-branes at $(-m, -n)$, so we may keep only the θ^2 projection and do not impose the θ projection. Similarly, only D3-branes with the third coordinate $p = 0$ are fixed under Ω_3, and thus are subject to Ω_3 projection. In the following we state the explicit projections for D3-branes at different θ^2 fixed points.

For D3-branes at $(0, 0, 0)$ point we have the projections

$$\begin{aligned} \mathbf{33} \quad \text{Gauge} \qquad & \lambda = \gamma_{\theta,3,(0,0,0)} \lambda \gamma^{-1}_{\theta,3,(0,0,0)} \; ; \qquad \lambda = -\gamma_{\Omega_3,3,(0,0,0)} \lambda^T \gamma^{-1}_{\Omega_3,3,(0,0,0)} \; ; \\ i^{th}\text{Chiral} \quad & \lambda = e^{2\pi i v_i} \gamma_{\theta,3,(0,0,0)} \lambda \gamma^{-1}_{\theta,3,(0,0,0)} \; ; \; \lambda = \pm \gamma_{\Omega_3,3,(0,0,0)} \lambda^T \gamma^{-1}_{\Omega_3,3,(0,0,0)} \; , \end{aligned} \tag{43}$$

with positive sign for $i = 1, 2$, and negative for $i = 3$.

For D3-branes at $(m, n, 0)$ with $(m, n) = (1, 0), (0, 1), (1, 1), (1, -1)$, we have the projections

$$\begin{aligned} \mathbf{33} \quad \text{Gauge} \qquad & \lambda = \gamma_{\theta^2,3,(m,n,0)} \; \lambda \; \gamma^{-1}_{\theta^2,3,(m,n,0)} \; ; \qquad \lambda = -\gamma_{\Omega,3,(m,n,0)} \; \lambda^T \; \gamma^{-1}_{\Omega,3,(m,n,0)} \; ; \\ i^{th}\text{Chiral} \quad & \lambda = e^{2\pi i 2 v_i} \; \gamma_{\theta^2,3,(m,n,0)} \; \lambda \; \gamma^{-1}_{\theta^2,3,(m,n,0)} \; ; \; \lambda = \pm \; \gamma_{\Omega,3,(0,0,0)} \; \lambda^T \; \gamma^{-1}_{\Omega,3,(0,0,0)} \; , \end{aligned} \tag{44}$$

with positive sign for $i = 1, 2$, and negative for $i = 3$. Other (m, n) fixed points are just θ-images of the above.

For D3-branes at $(0, 0, +1)$

$$\begin{aligned} \mathbf{33} \quad \text{Gauge} \qquad & \lambda = \gamma_{\theta,3,(0,0,+1)} \; \lambda \; \gamma^{-1}_{\theta,3,(0,0,+1)} \; ; \\ i^{th}\text{Chiral} \quad & \lambda = e^{2\pi i v_i} \; \gamma_{\theta,3,(0,0,+1)} \; \lambda \; \gamma^{-1}_{\theta,3,(0,0,+1)} \; \gamma^{-1}_{\Omega,3,(0,0,0)} \; . \end{aligned} \tag{45}$$

D3-branes at $p = -1$ are just Ω_3-images of the above.

Finally, for D3-branes at $(m, n, +1) = (0, 1, 1), (1, 0, 1), (1, 1, 1), (1, -1, 1)$, we have

$$\begin{aligned} \mathbf{33} \quad \text{Gauge} \qquad & \lambda = \gamma_{\theta^2,3,(m,n,+1)} \; \lambda \; \gamma^{-1}_{\theta^2,3,(m,n,+1)} \; ; \\ i^{th}\text{Chiral} \quad & \lambda = e^{2\pi i 2 v_i} \; \gamma_{\theta^2,3,(m,n,+1)} \; \lambda \; \gamma^{-1}_{\theta^2,3,(m,n,+1)} \; . \end{aligned} \tag{46}$$

Other $(m, n, +1)$ points are just θ-images of the above, and points $(m, n, -1)$ are Ω_3-images of the above.

Finally, we turn to the $7_3 3$ sector. There is one such sector for each point (m, n, p) at which D3-branes may sit. The massless states arise from D7_3- and D3-branes with identical

p. In performing the orbifold projection one should realize that at a point with coordinates (m,n) in the first two planes the θ action felt by the D7$_3$-branes depends on the Wilson lines along these directions. Again, we have to distinguish several cases.

For $(0,0,0)$, Ω_3 maps the 7_33 sector to the 37_3 sector, so we keep the former and do not impose the Ω_3 projection. We have

$$\mathbf{7_33}\quad \lambda = e^{-\pi i v_3}\ \gamma_{\theta,7_3,0}\ \lambda\ \gamma^{-1}_{\theta,3,(0,0,0)}\ . \tag{47}$$

At points $(m,n,0)$, Ω_3 maps the 7_33 sector to the 37_3 one, so we keep the former and do not impose the Ω_3 projection. Also, θ action maps the point $(m,n,0)$ to $(-m,-n,0)$, and we may restrict ourselves to $(m,n)=(1,0),(0,1),(1,1),(1,-1)$. The θ^2 projection is

$$\mathbf{7_33}\quad \lambda = e^{-\pi i 2v_3}\ (\gamma_{\theta^2,7_3,0}\ \gamma^{2m}_{W_1,7_3,0}\ \gamma^{2n}_{W_2,7_3,0})\ \lambda\ \gamma^{-1}_{\theta,3,(m,n,0)}\ . \tag{48}$$

At points $(0,0,p)$, Ω_3 maps the 7_33 sector to the 37_3 sector *at a different point* $(0,0,-p)$, so we may keep both the 37_3 and 7_33 sectors at $(0,0,1)$ and do not impose the Ω_3 projection. We have

$$\begin{aligned}
&\mathbf{7_33}\quad \lambda = e^{-\pi i v_3}\ \gamma_{\theta,7_3,+1}\ \lambda\ \gamma^{-1}_{\theta,3,(0,0,+1)}\ ;\\
&\mathbf{37_3}\quad \lambda = e^{-\pi i v_3}\ \gamma_{\theta,3,(0,0,+1)}\ \lambda\ \gamma^{-1}_{\theta,7_3,0}\ .
\end{aligned} \tag{49}$$

Finally, at points (m,n,p), we may keep both the 37_3 and 7_33 sectors for points with $(m,n)=(1,0),(0,1),(1,1),(1,-1)$ and $p=+1$, and do not impose the θ or Ω_3 projections. We have

$$\begin{aligned}
&\mathbf{7_33}\quad \lambda = e^{-\pi i 2v_3}\ (\gamma_{\theta^2,7_3,+1}\ \gamma^{2m}_{W_1,7_3,+1}\ \gamma^{2n}_{W_2,7_3,+1})\ \lambda\ \gamma^{-1}_{\theta,3,(m,n,+1)}\ ;\\
&\mathbf{37_3}\quad \lambda = e^{-\pi i 2v_3}\ \gamma_{\theta^2,3,(m,n,+1)}\ \lambda\ (\gamma_{\theta,7_3,+1}\ \gamma^{2m}_{W_1,7_3,+1}\ \gamma^{2n}_{W_2,7_3,+1})^{-1}\ .
\end{aligned} \tag{50}$$

V. MODELS

A. Systematic Construction of Models

In this Section, we develop an algorithm which allows us to systematically construct a large class of $\mathbf{Z_6}$ orientifold models that satisfy the algebraic and tadpole cancellation constraints.

In the $\mathbf{Z_6}$ orientifold model constructed in [4,6] which does not have Wilson lines, all the D5$_3$ branes are placed at the origin. The resulting gauge structure is $(U(6)\times U(4)\times U(4))^2$

from both D9- and D5_3 brane sector. To further break down the gauge structure to smaller groups, Wilson lines have to be introduced.

Our models in general include non-trivial discrete Wilson lines along the third complex plane, embedded both on D9- and D5_3-branes. The configuration becomes more intuitive if we perform a T-duality along this plane. In the T-dual picture, there are D7_3-branes sitting at three different fixed points in the third plane, $p = -1, 0, 1$. And there are D3-branes that sit at fixed points of all three complex planes, (m, n, p). The tadpole cancellation conditions in Eqn.(33) together with the group consistency conditions constraint the number of the branes at each fixed point and the gauge groups that arise from the set of branes.

Consider D7_3 branes at $p = 0$. Since $p = 0$ is a $\mathbf{C^3/Z_6}$ orientifold point, the action of θ twist takes the form of Eqn.(2). In addition, we have to solve the tadpole conditions (33). A simple possibility is to saturate the θ^2 tadpoles at the points $(m, n, 0)$ with $(m, n) \neq (0, 0)$ purely by the D7_3-brane contribution (so that no D3-branes are required there), satisfying $\mathrm{Tr}\,(\gamma_{\theta^2,7_3,0}) = 4$. We choose to put 8 $D7_3$ branes at $p = 0$, with

$$\gamma_{\theta,7_3,0} = \mathrm{diag}\,(e^{i\frac{\pi}{6}}\mathbf{1}_2, e^{i\frac{5\pi}{6}}\mathbf{1}_2, e^{i\frac{7\pi}{6}}\mathbf{1}_2, e^{i\frac{11\pi}{6}}\mathbf{1}_2). \tag{51}$$

In analogy with the analysis in [21], there exist other choices also satisfying the tadpole conditions, but we do not consider them here.

We now turn to tadpoles at $(0, 0, 0)$, which are not fully canceled by the D7_3-branes above. To cancel the remaining contribution, we introduce a set of $D3$ branes at $(0, 0, 0)$, with

$$\gamma_{\theta,3,(0,0,0)} = \mathrm{diag}\,(e^{i\frac{\pi}{6}}\mathbf{1}_2, e^{i\frac{5\pi}{6}}\mathbf{1}_2, e^{i\frac{7\pi}{6}}\mathbf{1}_2, e^{i\frac{11\pi}{6}}\mathbf{1}_2). \tag{52}$$

Out of the remaining 24 $D7_3$ branes left, we locate half of them at $p = 1$ and the other half at its orientifold image $p = -1$. The θ twist takes the general form of Eqn.(2)

$$\gamma_{\theta,7_3,1} = \mathrm{diag}\,(e^{\pi i\frac{1}{6}}\mathbf{1}_{N_1}, e^{\pi i\frac{3}{6}}\mathbf{1}_{N_2}, e^{\pi i\frac{5}{6}}\mathbf{1}_{N_3}, e^{\pi i\frac{7}{6}}\mathbf{1}_{N_4}, e^{\pi i\frac{9}{6}}\mathbf{1}_{N_5}, e^{\pi i\frac{11}{6}}\mathbf{1}_{N_6}), \tag{53}$$

where $\sum_{i=1}^{6} N_i = 12$. Their contributions to the tadpole associated with fixed point $(0, 0, 1)$ must be canceled by that from $D3$ branes sitting at the fixed point, as seen from Eqn.(33). The θ action on this set of $D3$ branes takes a similar form

$$\gamma_{\theta,3,(0,0,1)} = \mathrm{diag}\,(e^{\pi i\frac{1}{6}}\mathbf{1}_{M_1}, e^{\pi i\frac{3}{6}}\mathbf{1}_{M_2}, e^{\pi i\frac{5}{6}}\mathbf{1}_{M_3}, e^{\pi i\frac{7}{6}}\mathbf{1}_{M_4}, e^{\pi i\frac{9}{6}}\mathbf{1}_{M_5}, e^{\pi i\frac{11}{6}}\mathbf{1}_{M_6}), \tag{54}$$

where M_i is a different set of integers and their sum, which is the total number of $D3$ branes placed at $(0, 0, 1)$, is not fixed.

The rest of the $D3$ branes $(24 - 2\sum_{i=1}^{6} M_i)$ can be placed at fixed points (m, n, p), where $(m, n) \neq (0, 0)$. We also consider $p \neq 0$ as well, since tadpoles at $(m, n, 0)$ are already canceled. There are four types of points: $(1, 0, 1)$ and its 3 images [i.e. the θ^3 image $(-1, 0, 1)$, and their Ω_3 images, $(\pm 1, 0, -1)$]; $(0, 1, 1)$ and its 3 images; $(1, 1, 1)$ and its 3 images; and $(1, -1, 1)$ and its 3 images. These points are fixed under θ^2 only, so we need to specify its orbifold action, which takes the form:

$$\begin{aligned}
\gamma_{\theta^2,3,(1,0,1)} &= -\mathrm{diag}\,(\mathbf{1}_{i_1}, e^{i\frac{4\pi}{3}}\mathbf{1}_{i_2}, e^{i\frac{2\pi}{3}}\mathbf{1}_{i_3});\\
\gamma_{\theta^2,3,(0,1,1)} &= -\mathrm{diag}\,(\mathbf{1}_{j_1}, e^{i\frac{4\pi}{3}}\mathbf{1}_{j_2}, e^{i\frac{2\pi}{3}}\mathbf{1}_{j_3});\\
\gamma_{\theta^2,3,(1,1,1)} &= -\mathrm{diag}\,(\mathbf{1}_{k_1}, e^{i\frac{4\pi}{3}}\mathbf{1}_{k_2}, e^{i\frac{2\pi}{3}}\mathbf{1}_{k_3});\\
\gamma_{\theta^2,3,(1,-1,1)} &= -\mathrm{diag}\,(\mathbf{1}_{l_1}, e^{i\frac{4\pi}{3}}\mathbf{1}_{l_2}, e^{i\frac{2\pi}{3}}\mathbf{1}_{l_3}),
\end{aligned} \tag{55}$$

where $\sum_{n=1}^{3}(2i_n + 2j_n + 2k_n + 2l_n) = 12 - \sum_{i=1}^{6} M_i$.

In addition, we also consider the possibility of general order three discrete Wilson lines in the first and second complex planes. The Wilson line in the first complex plane takes the form of Eqn.(9) with three parameters $m_{1,2,3}$, and the Wilson line in the second complex plane takes the form of Eqn.(12) with 12 parameters x_i $(i = 1, \ldots, 12)$.

We can now calculate the traces of the γ-matrices and express the tadpole cancellation conditions Eqs.(33) in terms of the set of parameters N_n, M_n, i_n, j_n, k_n, l_n, m_n, x_n. Since the number of equations is less than the number of parameters, we search through the whole parameter space for allowed solutions. There is a seemingly large number of solutions, however, many solutions are related by symmetries of the construction, and are therefore equivalent. Our results show that the number of inequivalent solutions is limited.

Let us briefly discuss some of these equivalences. A transformation leaving the full spectrum of the theory invariant (including massive states) is the following: Multiply the $\mathbf{Z_6}$ Chan-Paton matrices γ_{θ^k} of all D-branes at $z_3 = +1$ by a constant brane-independent phase $e^{ik2\pi n/6}$, where $n = 1 \ldots 5$ (and by the conjugated phase in the orientifold images at $z_3 = -1$), leaving the Wilson lines unchanged. Models related by this transformation are completely equivalent. A second transformation which leaves the full theory invariant is to conjugate the orbifold and Wilson line Chan-Paton matrices for all D-branes at $z_3 = \pm 1$. Since matrices at $z_3 = +1$ and their orientifold images are conjugated of each other, the above operation is equivalent to the geometric symmetry of reflecting the models with respect to the plane $z_3 = 0$.

Imposing these equivalences, the number of solutions reduces drastically. In particular, we find that among the whole set of solutions only a few have a potential to give semi-realistic

models, i.e. those that have a gauge structure $SU(3) \times SU(2)^i \times U(1)^j$ as a subgroup.

Interestingly enough, we found only a few inequivalent classes of semi-realistic models containing a gauge structure of $U(3) \times U(2)^2 \times U(1)$ within a single D-brane sector (an interesting situation to obtain family replication of the spectrum). It arises from a set of D3 branes located at the fixed point $(0,0,1)$, or its T-dual version. The Chan-Paton matrices for $\gamma_{\theta,7_3,1}$ and $\gamma_{\theta,3,(0,0,1)}$ take the form

$$\begin{aligned} \gamma_{\theta,7_3,1} &= \mathrm{diag}\,(e^{i\frac{\pi}{6}}\mathbf{1}_2, e^{i\frac{3\pi}{6}}\mathbf{1}_3, e^{i\frac{5\pi}{6}}\mathbf{1}_4, e^{i\frac{7\pi}{6}}\mathbf{1}_1, e^{i\frac{11\pi}{6}}\mathbf{1}_2)\ ; \\ \gamma_{\theta,3,(0,0,1)} &= \mathrm{diag}\,(e^{i\frac{\pi}{6}}\mathbf{1}_1, e^{i\frac{7\pi}{6}}\mathbf{1}_2, e^{i\frac{11\pi}{6}}\mathbf{1}_3, e^{i\frac{11\pi}{6}}\mathbf{1}_2). \end{aligned} \tag{56}$$

The configuration and the Chan-Paton matrices of the remaining D3-branes and the Wilson line actions in the model are listed in Table I. Using the transformations above we can generate other models with seemingly different Chan-Paton matrices, but with completely equivalent spectra.

Moreover, close inspection of Table I reveals that some of these solutions are also related by further symmetries of the model, associated with modular transformations in the four-torus associated with the first two complex planes. For instance, the exchange of these complex planes has a non-trivial action on fixed points [mapping (m,n,p) to (n,m,p)] and on Wilson lines [exchanging $\gamma_{W_1,7_3}$ and $\gamma_{W_2,7_3}$], and allows one to relate, e.g., the third and fourth model, or the sixth and eighth model in Table I. Other modular transformations allow for less obvious equivalences. For instance, there exists a transformation mapping the fixed point (m,n,p) to $(m+n,n,p)$, and acting on Wilson lines as

$$\gamma_{W_1,7_3,1} \to \gamma_{W_1,7_3,1} \quad ; \quad \gamma_{W_2,7_3,1} \to \gamma_{W_2,7_3,1}\gamma^{-1}_{W_1,7_3,1}\ . \tag{57}$$

This allows one to relate models like the second and third, or like the fifth and sixth in Table I. Employing all the modular transformation equivalences, we find there are only two distinct solutions with the above mentioned gauge structure: the first contains two D3-branes placed at one fixed point $(m,n,1)$ with $(m,n) \neq (0,0)$, while the second involves two such fixed points, with one D3-brane sitting at each point. They correspond to the two equivalence classes of the models in Table I (which are separated by a double line).

In the following Subsection, we study in more detail the gauge structure and the matter spectrum of the first kind of the semi-realistic models, with two D3-branes at one fixed point. The second model can be analyzed analogously, and leads to very similar phenomenology.

However, before doing so, we would like to remark that tadpole cancellation constraints do not allow for a realistic gauge structure arising from D3-branes at the $\mathbf{C^3/Z_3}$ orbifold points. Solutions with the maximal allowed number of D3-branes placed at $\mathbf{Z_3}$ fixed points

(i_1, i_2, i_3)	(j_1, j_2, j_3)	(k_1, k_2, k_3)	(l_1, l_2, l_3)	(m_1, m_2, m_3)	$(x_1, x_2, \ldots, x_9)$
$(0,0,0)$	$(0,0,0)$	$(0,0,0)$	$(1,1,0)$	$(0,0,1)$	$(0,0,0,0,0,0,0,1,0)$
$(0,0,0)$	$(0,0,0)$	$(1,1,0)$	$(0,0,0)$	$(0,0,1)$	$(0,0,0,0,0,0,0,0,1)$
$(0,0,0)$	$(1,1,0)$	$(0,0,0)$	$(0,0,0)$	$(0,0,1)$	$(0,0,0,0,0,0,0,0,0)$
$(1,1,0)$	$(0,0,0)$	$(0,0,0)$	$(0,0,0)$	$(0,0,0)$	$(0,0,0,0,0,0,1,0,0)$
$(0,0,0)$	$(0,0,0)$	$(0,0,1)$	$(0,0,1)$	$(0,0,1)$	$(0,0,0,0,0,0,1,0,0)$
$(0,0,0)$	$(0,0,1)$	$(0,0,0)$	$(0,0,1)$	$(0,0,1)$	$(0,0,0,0,0,0,1,0,1)$
$(0,0,0)$	$(0,0,1)$	$(0,0,1)$	$(0,0,0)$	$(0,0,1)$	$(0,0,0,0,0,0,1,1,0)$
$(0,0,1)$	$(0,0,0)$	$(0,0,0)$	$(0,0,1)$	$(0,0,2)$	$(0,0,0,0,0,0,0,0,1)$
$(0,0,1)$	$(0,0,0)$	$(0,0,1)$	$(0,0,0)$	$(0,0,2)$	$(0,0,0,0,0,0,0,1,0)$
$(0,0,1)$	$(0,0,1)$	$(0,0,0)$	$(0,0,0)$	$(0,0,2)$	$(0,0,0,0,0,0,0,1,1)$

TABLE I. A set of the solutions for a semi-realistic model $U(3) \times U(2)^2 \times U(1)$ arising from the D3 brane sector.

correspond to six D3-branes at such orbifold points. However, as a result of strong constraints from tadpole cancellation conditions, the gauge structure arising form these D3-branes is $U(2)^3$. Therefore, N=1 supersymmetric solutions of the $\mathbf{Z_6}$ orientifold model do not reproduce the local configurations with realistic gauge group structure at $\mathbf{Z_3}$ fixed points, such as studied in [18]. However, in Subsection V C we show how the introduction of anti-branes, which break supersymmetry, allows for a realistic gauge groups arising from D3-branes at $\mathbf{Z_3}$ orbifold points.

B. A semi-realistic model

In this section we shall focus on the model with the semi-realistic gauge group structure. This model can be obtained with the following choice of values for the integer parameters defined in Subsection V A,

$$\begin{aligned} &N_1 = 2, \quad N_2 = 3, \quad N_3 = 4, \quad N_4 = 1, \quad N_5 = 0, \quad N_6 = 2; \\ &M_1 = 1, \quad M_2 = 0, \quad M_3 = 0, \quad M_4 = 2, \quad M_5 = 3, \quad M_6 = 2; \\ &j_1 = 1, \quad j_2 = 1, \quad j_3 = 0; \\ &m_1 = 0, \quad m_2 = 0, \quad m_3 = 1, \end{aligned} \tag{58}$$

while $i_n = k_n = l_n = x_n = 0$. Namely, the model has 8 D3-branes at the origin, 8 D7_3-branes at $p = 0$, 12 D7_3 branes at $p = 1$ and 12 at its orientifold image $p = -1$. In addition, there are 2 $D3$-branes at the point $(0, 1, 1)$ and its three images. There is also one order-three Wilson line acting on the first complex plane.

The gauge group on the D7_3-brane sector at $p = 1$, before the Wilson line projection is imposed, is [with grouping of the integer entries as $(N_1, N_2, N_3, N_4, N_5, N_6)$]:

$$G_{\theta,7_3,1} = U(2) \times U(3) \times U(4) \times U(1) \times U(2) \ . \tag{59}$$

The Wilson line breaks $U(4)$ to $U(3) \times U(1)'$ and the first $U(2)$ to $U(1) \times U(1)''$, and further breaks $U(1)' \times U(1)''$ to the diagonal combination $U(1)_{diag}$. The remaining group is

$$G^{\rm Wilson}_{\theta,7_3,1} = U(2) \times U(3) \times U(3) \times U(1) \times U(1) \times U(1)_{diag}. \tag{60}$$

The 7_37_3 spectrum before the Wilson line projection is

$$\begin{aligned} 2 \ \times \ [\ &(\mathbf{2}, \overline{\mathbf{3}}, \mathbf{1}, \mathbf{1})_{[1,-1,0,0,0]} + (\mathbf{1}, \mathbf{3}, \overline{\mathbf{4}}, \mathbf{1})_{[0,1,-1,0,0]} + (\mathbf{1}, \mathbf{1}, \mathbf{4}, \mathbf{1})_{[0,0,1,-1,0]} + (\overline{\mathbf{2}}, \mathbf{1}, \mathbf{1}, \mathbf{2})_{[-1,0,0,0,1]} \ ] \ + \\ &+ (\overline{\mathbf{2}}, \mathbf{1}, \mathbf{4}, \mathbf{1})_{[-1,0,1,0,0]} + (\mathbf{1}, \overline{\mathbf{3}}, \mathbf{1}, \mathbf{1})_{[0,-1,0,1,0]} + (\mathbf{1}, \mathbf{1}, \mathbf{1}, \mathbf{2})_{[0,0,0,-1,1]} + (\mathbf{1}, \mathbf{3}, \mathbf{1}, \overline{\mathbf{2}})_{[0,1,0,0,-1]} \ , \end{aligned} \tag{61}$$

where we put a bar over the fundamentals of $SU(2)$ which have -1 charge under the corresponding $U(1)$ in $U(2)$.

After the Wilson line projection, the spectrum in this sector is

$$\begin{aligned} A_1^{(7)}, B_1^{(7)} &: \ 2 \ \times \ (\mathbf{2}, \overline{\mathbf{3}}, \mathbf{1})_{[1,-1,0,0,0,0]}; \\ A_2^{(7)}, B_2^{(7)} &: \ 2 \ \times \ (\mathbf{1}, \mathbf{3}, \overline{\mathbf{3}})_{[0,1,-1,0,0,0]}; \\ A_3^{(7)}, B_3^{(7)} &: \ 2 \ \times \ (\mathbf{1}, \mathbf{1}, \mathbf{3})_{[0,0,1,-1,0,0]}; \\ A_6^{(7)}, B_6^{(7)} &: \ 2 \ \times \ (\overline{\mathbf{2}}, \mathbf{1}, \mathbf{1})_{[-1,0,0,0,1,0]}; \\ C_2^{(7)} &: \qquad (\mathbf{1}, \mathbf{3}, \mathbf{1})_{[0,1,0,0,-1,0]}; \\ C_3^{(7)} &: \qquad (\overline{\mathbf{2}}, \mathbf{1}, \mathbf{3})_{[-1,0,1,0,0,0]}; \\ C_4^{(7)} &: \qquad (\mathbf{1}, \overline{\mathbf{3}}, \mathbf{1})_{[0,-1,0,1,0,0]}; \\ C_6^{(7)} &: \qquad (\mathbf{1}, \mathbf{1}, \mathbf{1})_{[0,0,0,-1,1,0]} \ , \end{aligned} \tag{62}$$

where the representations are under $SU(2) \times SU(3) \times SU(3)$, and the subscripts correspond to $U(1)$ charges. The superscripts (7) denote the states arising in a D7-brane sector.

The gauge group on the $D3$-sector at the point $(0, 0, 1)$ (and its orientifold image) is of the form:

$$G_{\theta,3,(0,0,1)} = U(1) \times U(2) \times U(3) \times U(2) \ . \tag{63}$$

The spectrum of chiral multiplets in this 33 sector is

$$\begin{aligned}
&A_4^{(3)}, B_4^{(3)} : \ 2 \ \times \ (\mathbf{2}, \overline{\mathbf{3}}, \mathbf{1})_{[0,1,-1,0]}; \\
&A_5^{(3)}, B_5^{(3)} : \ 2 \ \times \ (\mathbf{1}, \mathbf{3}, \overline{\mathbf{2}})_{[0,0,1,-1]}; \\
&A_6^{(3)}, B_6^{(3)} : \ 2 \ \times \ (\mathbf{1}, \mathbf{1}, \mathbf{2})_{[-1,0,0,1]}; \\
&\quad C_1^{(3)} \qquad\quad (\mathbf{1}, \overline{\mathbf{3}}, \mathbf{1})_{[1,0,-1,0]}; \\
&\quad C_6^{(3)} \qquad\quad (\overline{\mathbf{2}}, \mathbf{1}, \mathbf{2})_{[0,-1,0,1]} \ .
\end{aligned} \tag{64}$$

The superscripts (3) denote the corresponding fields arise from the D3-brane sector.

In the 37_3 and 7_33 sectors, we obtain

$$\begin{aligned}
\mathbf{37_3} \ \ & D_1^{(37)} : \ \ (\mathbf{1}, \mathbf{1}, \mathbf{1})_{[1,0,0,0]} \times (\mathbf{1}, \overline{\mathbf{3}}, \mathbf{1})_{[0,-1,0,0,0,0]} \ ; \\
& D_5^{(37)} : \ \ (\mathbf{1}, \mathbf{3}, \mathbf{1})_{[0,0,1,0]} \times (\mathbf{1}, \mathbf{1}, \mathbf{1})_{[0,0,0,0,-1,0]} \ ; \\
& \tilde{D}_5^{(37)} : \ \ (\mathbf{1}, \mathbf{3}, \mathbf{1})_{[0,0,1,0]} \times (\mathbf{1}, \mathbf{1}, \mathbf{1})_{[0,0,0,0,0,-1]} \ ; \\
& D_6^{(37)} : \ \ (\mathbf{1}, \mathbf{1}, \mathbf{2})_{[0,0,0,1]} \times (\overline{\mathbf{2}}, \mathbf{1}, \mathbf{1})_{[-1,0,0,0,0,0]} \ ; \\
\mathbf{7_33} \ \ & E_3^{(73)} : \ \ (\overline{\mathbf{2}}, \mathbf{1}, \mathbf{1})_{[0,-1,0,0]} \times (\mathbf{1}, \mathbf{1}, \mathbf{3})_{[0,0,1,0,0,0]} \ ; \\
& \tilde{E}_3^{(73)} : \ \ (\overline{\mathbf{2}}, \mathbf{1}, \mathbf{1})_{[0,-1,0,0]} \times (\mathbf{1}, \mathbf{1}, \mathbf{1})_{[0,0,0,0,0,1]} \ ; \\
& E_4^{(73)} : \ \ (\mathbf{1}, \overline{\mathbf{3}}, \mathbf{1})_{[0,0,-1,0]} \times (\mathbf{1}, \mathbf{1}, \mathbf{1})_{[0,0,0,1,0,0]} \ ; \\
& E_6^{(73)} : \ \ (\mathbf{1}, \mathbf{1}, \mathbf{1})_{[-1,0,0,0]} \times (\mathbf{1}, \mathbf{1}, \mathbf{1})_{[0,0,0,0,1,0]} \ ; \\
& \tilde{E}_6^{(73)} : \ \ (\mathbf{1}, \mathbf{1}, \mathbf{1})_{[-1,0,0,0]} \times (\mathbf{1}, \mathbf{1}, \mathbf{1})_{[0,0,0,0,0,1]} \ ,
\end{aligned}$$

where the two parts for each state give the quantum numbers under the D3- and D7_3-brane gauge groups.

The D3-branes at the point $(0, 1, 1)$ (and its images) produce a gauge group $G_{\theta,3,(0,1,1)} = U(1) \times U(1)$. In the 33 sector, we obtain the multiplets

$$A_2^{(3')}, B_2^{(3')}, C_2^{(3')} : \ \ 3 \ \times \ \mathbf{1}_{[-1,1]} \ , \tag{65}$$

where we use a prime to distinguish this D3-brane sector from the previous one. In the 37_3 and 7_33 sectors we obtain chiral multiplets

$$\begin{aligned}
\mathbf{37_3} \ \ & D_1^{(3'7)} : \ \ \mathbf{1}_{[1,0]} \times (\mathbf{1}, \mathbf{1}, \overline{\mathbf{3}})_{[0,0,-1,0,0,0]} \ ; \\
& \tilde{D}_1^{(3'7)} : \ \ \mathbf{1}_{[1,0]} \times (\mathbf{1}, \mathbf{1}, \mathbf{1})_{[0,0,0,0,0,0,-1]} \ ; \\
& G_1^{(3'7)} : \ \ \mathbf{1}_{[1,0]} \times (\mathbf{1}, \mathbf{1}, \mathbf{1})_{[0,0,0,0,0,-1,0]} \ ; \\
& \tilde{G}_1^{(3'7)} : \ \ \mathbf{1}_{[1,0]} \times (\mathbf{1}, \mathbf{1}, \mathbf{1})_{[0,0,0,0,0,0,-1]} \ ; \\
& D_3^{(3'7)} : \ \ \mathbf{1}_{[0,1]} \times (\mathbf{1}, \overline{\mathbf{3}}, \mathbf{1})_{[0,-1,0,0,0,0]} \ ;
\end{aligned}$$

$$
\begin{aligned}
\mathbf{7_3 3}\ \ E_1^{(73')} &: \ \ \mathbf{1}_{[-1,0]} \times (\mathbf{2},\mathbf{1},\mathbf{1})_{[1,0,0,0,0,0]} \ ; \\
E_3^{(73')} &: \ \ \mathbf{1}_{[0,-1]} \times (\mathbf{1},\mathbf{1},\mathbf{3})_{[0,0,1,0,0,0]} \ ; \\
\tilde{E}_3^{(73')} &: \ \ \mathbf{1}_{[0,-1]} \times (\mathbf{1},\mathbf{1},\mathbf{1})_{[0,0,0,0,0,1]} \ ; \\
E_4^{(73')} &: \ \ \mathbf{1}_{[-1,0]} \times (\mathbf{1},\mathbf{1},\mathbf{1})_{[0,0,0,1,0,0]} \ ; \\
E_6^{(73')} &: \ \ \mathbf{1}_{[0,-1]} \times (\mathbf{1},\mathbf{1},\mathbf{1})_{[0,0,0,0,1,0]} \ ; \\
\tilde{E}_6^{(73')} &: \ \ \mathbf{1}_{[0,-1]} \times (\mathbf{1},\mathbf{1},\mathbf{1})_{[0,0,0,0,0,1]} \ . \qquad (66)
\end{aligned}
$$

To complete the model, we now turn to the D7_3-branes placed at $p = 0$ and the D3-branes placed at the origin. Each of them gives rise to the gauge group

$$G_{\theta,7_3,0} = G_{\theta,3,(0,0,0)} = U(2) \times U(2) \ . \qquad (67)$$

In the $7_3 7_3$ sector we obtain chiral multiplets in the representation

$$2 \ \times \ [\ (\mathbf{1},\mathbf{1})_{[0,2]} + (\mathbf{1},\mathbf{2})_{[-2,0]}\ ] + (\overline{\mathbf{2}},\mathbf{2})_{[-1,1]} \ . \qquad (68)$$

In the 33 sector we obtain the same type of spectrum. The 37_3 and $7_3 3$ are related by the orientifold projection, so it suffices to compute just the former, which produces fields

$$(\overline{\mathbf{2}},\mathbf{1})_{[-1,0]} \times (\overline{\mathbf{2}},\mathbf{1})_{[-1,0]} + (\mathbf{1},\mathbf{2})_{[0,1]} \times (\mathbf{1},\mathbf{2})_{[0,1]} \ . \qquad (69)$$

It is easy to check that all cubic non-Abelian anomalies cancel.

The full superpotential for fields arising from branes at $z_3 = 1$ is given by

$$
\begin{aligned}
W = {} & A_6^{(7)} B_1^{(7)} C_2^{(7)} - B_6^{(7)} A_1^{(7)} C_2^{(7)} + A_1^{(7)} B_2^{(7)} C_3^{(7)} - B_1^{(7)} A_2^{(7)} C_3^{(7)} + A_2^{(7)} B_3^{(7)} C_4^{(7)} - B_2^{(7)} A_3^{(7)} C_4^{(7)} + \\
& + A_5^{(3)} B_6^{(3)} C_1^{(3)} - B_5^{(3)} A_6^{(3)} C_1^{(3)} + A_4^{(3)} B_5^{(3)} C_6^{(3)} - B_4^{(3)} A_5^{(3)} C_6^{(3)} + \\
& + D_5^{(37)} E_6^{(73)} C_1^{(3)} + E_4^{(73)} D_5^{(37)} C_6^{(7)} + E_6^{(73)} D_1^{(37)} C_2^{(7)} + \\
& + C_2^{(3')} D_1^{(3'7)} E_3^{(73')} + C_2^{(3')} \tilde{D}_1^{(3'7)} \tilde{E}_3^{(73')} + C_2^{(3')} G_1^{(3'7)} E_6^{(73')} + C_2^{(3')} \tilde{G}_1^{(3'7)} \tilde{E}_6^{(73')} \ . \qquad (70)
\end{aligned}
$$

As usual in type IIB orientifold models, mixed $U(1)$ triangle anomalies do not vanish, but are canceled by a generalized Green-Schwarz mechanism mediated by closed string twisted modes [20] (see [22] for the six-dimensional version of this effect). The anomalous $U(1)$'s gain a mass of the order of the string scale [23], and disappear from the low-energy physics. It is therefore important to determine the non-anomalous (and therefore light) $U(1)$'s in the model.

The non-anomalous U(1)'s can be found by directly computing the matrix of mixed $U(1)$-non-Abelian anomalies. We order the gauge factors as they arise in

$$G^{Wilson}_{\theta,7_3,1} \times G_{\theta,3,(0,0,1)} \times G_{\theta,3,(0,1,1)} \ , \tag{71}$$

and denote each $U(1)$ generator by Q_i, i=1,...,12. Denoting by A_{ij} the mixed $Q_i - SU(N_j)^2$ anomaly, non-anomalous $U(1)$'s correspond to zero eigenvalue modes in this matrix. Namely, linear combinations $Q^{(k)} = \sum_i \frac{c_i^{(k)}}{N_i} Q_i$ satisfying $\sum_i \frac{c_i^{(k)}}{N_i} A_{ij} = 0$. In our model there are four independent non-anomalous $U(1)$'s, whose 12-dimensional vector of coefficients (c_i) are given by

$$\begin{aligned} c^{(1)} &= (-1,0,0,1,0,0;1,-1,0,0;0,0)\ ; \\ c^{(2)} &= (0,0,0,0,1,1;0,0,0,-1;1,1)\ ; \\ c^{(3)} &= (1,1,0,0,1,0;-1,1,0,0;0,0)\ ; \\ c^{(4)} &= (1,1,1,0,0,0;0,1,1,1;0,0)\ . \end{aligned} \tag{72}$$

Clearly, any linear combination of these is also non-anomalous. For instance, there exists one non-anomalous $U(1)$ arising only from D7_3-branes at $z_3 = +1$, without any D3-brane component. Its vector of components is obtained by adding the first and third vectors above, giving

$$(0,1,0,1,1,0;0,0,0,0;0,0)\ , \tag{73}$$

which corresponds to $Q = \frac{2}{3}Q_2 + Q_4 + Q_5$.

In an attempt to identify possible candidates for $U(1)_Y$ hypercharge in the model, we consider the following scenario. Fields A_4, B_4 are taken to be quark singlets, while A_5, B_5 are identified as quark doublets, A_6, B_6 are lepton doublets and C_6 is the Higgs. Therefore the sector of D3-branes at the point $(0,0,1)$ gives rise to a left-right symmetric semi-realistic sector with group $SU(3)_{color} \times SU(2)_L \times SU(2)_R$, and two quark-lepton families. In order to obtain correct hypercharge assignments after breaking of $SU(2)_R$, we need a correct $(B\text{-}L)$-charge Q_{B-L} to form the linear combination $Q_Y = Q_{B-L} + 2I_R$. Defining

$$Q_{B-L} = a \times c^{(1)} + b \times c^{(2)} + c \times c^{(3)} + d \times c^{(4)}\ . \tag{74}$$

and requiring that Q_{B-L} charge assignments are correct, one arrives at the following two constraints

$$a = b + c \ \ ; \ \ d = 3b - 2. \tag{75}$$

A simple solution is $b = c = 0$, leading to $Q_{B-L} = -2 \times c^{(4)}$, which can be cast in the form

$$Q_{B-L} = (\frac{1}{2}Q_1 + \frac{1}{3}Q_2 + \frac{1}{3}Q_3) + (\frac{1}{2}Q_8 + \frac{1}{3}Q_9 + \frac{1}{2}Q_{10})\ , \tag{76}$$

where the first bracket arises from $D7_3$-brane gauge factors, and the second one from D3-branes gauge factors located at $(0,0,1)$. Notice that, as opposed to the realistic models in [18,24], the hypercharge in this model arises from $U(1)$ linear combinations of different brane sectors. It would be interesting to gain a better understanding of the origin of such non-anomalous $U(1)$'s as (B-L) and/or hypercharge candidates and their phenomenological implications.

We refrain from entering a more detailed discussion of the phenomenological properties of this mode, e.g., the charge assignments of fields in other sectors, or the study of superpotential couplings, which is a subject of further studies [19]. In the next Subsection we turn to the discussion of orientifold models with broken supersymmetry.

C. A semi-realistic model with anti-branes

It is possible to see that the main obstruction to obtain three-family models with realistic gauge groups in the framework we have described is the limited amount of available branes. For instance, following the approach in [18], one may try to obtain such a realistic sector from a set of six D3-branes at one of the $\mathbf{C^3/Z_3}$ orbifold points. Since such points have images under θ^3 and Ω_3, the number of D3-branes involved is 24. Counting also the D3-branes at $(0,0,0)$ whose minimum number is 8, we saturate the total number of available 32 D3-branes. However, all models built in this manner with the requirement that the set of six D3-branes at one of the $\mathbf{C^3/Z_3}$ orbifold gives rise to realistic gauge structure, i.e., $SU(3)\times SU(2)\times U(1)$, contain non-zero tadpoles at some of the additional $\mathbf{C^3/Z_3}$ orbifold points, arising from $D7_3$-brane disks. Since all 32 D3-branes have been already placed at other points, the tadpoles remain uncancelled, rendering such models inconsistent.

The introduction of anti-branes in the construction of orientifolds [25] (see also [24,26] for further developments) allows one to build models where, e.g., the number of D3-branes N is larger than 32, the excess of untwisted charge being compensated by $N-32$ anti-D3-branes (denoted $\overline{\rm D3}$-branes). In this subsection we would like to briefly discuss the construction of a semi-realistic orientifold, with Pati-Salam gauge group $SU(3)_{color}\times SU(2)_L\times SU(2)_R\times U(1)_{B-L}$ and three families of quarks and leptons with correct gauge quantum numbers. This sector arises from a set of D3-branes sitting at a $\mathbf{C^3/Z_3}$ orbifold point, and is identical to those studied in [18].

We start by placing 20 $D7_3$-branes at $z_3=0$ with

$$\gamma_{\theta,7_3,0}=\mathrm{diag}\,(e^{\pi i\frac{1}{6}}\mathbf{1}_4,e^{\pi i\frac{3}{6}}\mathbf{1}_2,e^{\pi i\frac{5}{6}}\mathbf{1}_4,e^{\pi i\frac{7}{6}}\mathbf{1}_4,e^{\pi i\frac{9}{6}}\mathbf{1}_2,e^{\pi i\frac{11}{6}}\mathbf{1}_4)\ . \tag{77}$$

This choice differs from (51) only by a traceless piece, so the analysis is similar to that described in Subsection V A. In particular, all crosscap tadpoles are canceled at points $(m, n, 0)$, except at the origin. In order to cancel the latter, we choose to introduce four $\overline{\mathrm{D3}}$-branes with

$$\gamma_{\theta,\overline{3},(0,0,0)} = \mathrm{diag}\,(e^{\pi i\frac{3}{6}}\mathbf{1}_2, e^{\pi i\frac{9}{6}}\mathbf{1}_2)\ . \tag{78}$$

$\overline{\mathrm{D3}}$-branes carry RR charges opposite to those of D3-branes, hence their contribution to tadpoles is opposite to that of a set of D3-branes with the same Chan-Paton matrix. Using this fact, the above choice is seen to cancel the tadpole at $(0, 0, 0)$.

Up to this point we have introduced 20 $\mathrm{D7}_3$-branes and 4 $\overline{\mathrm{D3}}$-branes, so cancellation of untwisted tadpoles requires the introduction of 12 additional $\mathrm{D7}_3$-branes, and 36 D3-branes, split symmetrically between the points at $z_3 = 1$ and its Ω_3 images. The discussion is analogous to that in Subsection V A, differing only in the total number of branes allowed.

We locate six $\mathrm{D7}_3$-branes at $z_3 = 1$ (and the remaining 6 at its Ω_3-image), with

$$\gamma_{\theta,7_3,1} = \mathrm{diag}\,(e^{\pi i\frac{1}{6}}, e^{\pi i\frac{3}{6}}, e^{\pi i\frac{5}{6}}, e^{\pi i\frac{7}{6}}, e^{\pi i\frac{9}{6}}, e^{\pi i\frac{11}{6}})\ , \tag{79}$$

that is $N_1 = N_2 = N_3 = N_4 = N_5 = N_6 = 2$ in (53). Since this matrix is traceless, we may choose to place no D3-branes at $(0, 0, 1)$, i.e. $M_i = 0$ in (54). In order to have nontrivial sectors at the $\mathbf{C^3/Z_3}$ orbifold points, we introduce an order three Wilson line along the first plane on the $\mathrm{D7}_3$-branes, corresponding to $m_1 = m_3 = 0$, $m_2 = 1$ in (9), so in the basis diagonalizing $\gamma_{\theta^2,7_3,+1}$ and $\gamma_{W_1,7_3,+1}$ it reads

$$\tilde{\gamma}_{W_1,7_3,+1} = \mathrm{diag}\,(1, e^{2\pi i\frac{1}{3}}, 1, 1, e^{2\pi i\frac{2}{3}}, 1)\ . \tag{80}$$

Finally, we turn to the choice of location and Chan-Paton factors for D3-branes (55), with the modified constraint $\sum_n(2i_n + 2j_n + 2k_n + 2l_n) = 18$. Fixed points of the form $(0, n, 1)$ do not feel the Wilson line, and their tadpoles cancel without the introduction of D3-branes sitting at them, hence $j_n = 0$. At the remaining points, the D3-brane Chan-Paton trace should be -1, so we may choose $k_1 = l_1 = 1$, $k_2 = k_3 = l_2 = l_3 = 0$, $i_1 = 3$, $i_2 = i_3 = 2$.

The computation of the open string massless spectrum is lengthy, but straightforward. In any event, the important aspect we would like to point out is that the local behavior near the fixed point $(1, 0, 1)$ (and its images) is exactly as in the models in [24,18], hence this D3-brane sector leads automatically to a three-family $SU(3)_{color} \times SU(2)_L \times SU(2)_R \times U(1)_{B-L}$. The $U(1)_{B-L}$ arises from the unique non-anomalous linear combination of $U(1)$'s, purely in the D3-brane sector, and whose charge is given by

$$Q_{B-L} = -2(\frac{1}{3}Q_{U(3)} + \frac{1}{2}Q_{U(2)} + \frac{1}{2}Q_{U(2)}). \tag{81}$$

Also note that, even though the full model is non-supersymmetric due to the presence of the anti-branes, the latter sit at $z_3 = 0$, i.e. are separated from the semi-realistic sector, which enjoys $N = 1$ supersymmetry, only broken at higher orders by the hidden anti-brane sector.

The spectrum charged under gauge factors in this sector of D3-branes is

$$\begin{aligned}
& SU(3) \times SU(2)_L \times SU(2)_R \times U(1)_{B-L} \\
\mathbf{33} \;:\quad & 3 \;\times\; [\; (3,2,1)_{1/3} + (1,2,2)_0 + (\overline{3},1,1)_{-1/3} \;] \;; \\
\mathbf{37_3} \;:\quad & 3 \;\times\; [\; (3,1,1)_{-2/3} + (1,2,1)_{-1} \;] \;; \\
\mathbf{7_33} \;:\quad & 3 \;\times\; [\; (1,1,2)_1 + (\overline{3},1,1)_{2/3} \;] \;.
\end{aligned} \tag{82}$$

The three copies of fields in the mixed sector actually differ in their charges under the $D7_3$-brane gauge group $U(1)^3$, not shown here. In fact, we expect these additional $U(1)$'s to be anomalous, and therefore broken and not present at low energies. We will not pursue their discussion here.

Finally note that the model we have just constructed is in principle unstable against moving some of the D3-branes at $(1, 0, 1)$ and annihilating them with the $\overline{\text{D3}}$-branes at the origin. This instability is identical to that in the models in [24], but it can be avoided in more involved constructions [18]. In any event, our purpose was to illustrate how the construction of realistic models using the $\mathbf{Z_6}$ orientifold is possible and relatively easy once the restriction of supersymmetry is relaxed.

VI. CONCLUSIONS

In this paper we set out to develop techniques to construct consistent N=1 supersymmetric four-dimensional solutions of open (Type I) string theory compactified on $\mathbf{Z_N}$ and $\mathbf{Z_M} \times \mathbf{Z_N}$ symmetric orientifolds, *with general (continuous and discrete) Wilson lines*. In particular, our approach advances the techniques beyond the special examples of discrete [6,8,9,16] and continuous [6,5,17] Wilson lines. We have provided explicit solutions for the algebraic consistency conditions for discrete and continuous Wilson lines along complex planes twisted by an order six action. We have also studied the tadpole consistency conditions on the $\mathbf{Z_6}$ orientifold with general Wilson lines, and found explicit solution to this set of constraints, leading to interesting N=1 four-dimensional string vacua. And we would like to emphasize that our techniques in the construction of Wilson lines are general and applicable to other models.

In constructing models with Wilson lines we have heavily employed the geometrical interpretation of discrete Wilson line solutions in the T-dual picture as sets of branes located at the orbifold fixed points. In the T-dual picture the algebraic consistency conditions become constraints for the locations of these branes that are consistent with the orbifold and orientifold symmetries. We have also shown that the tadpole cancellation conditions for such T-dual models are related by a discrete Fourier transform. This useful trick allows one to obtain tadpoles in T-dual models without the need of directly computing them, and illuminates the detailed relation between brane positions and Wilson lines in orbifold models.

The second major motivation for advancing this program is phenomenological. Models with discrete Wilson lines naturally provide smaller gauge group structures (associated with the set of branes located at the orbifold points), and thus could potentially lead to gauge sectors with the ingredients of the standard model. However, previous four-dimensional N=1 supersymmetric Type I models (with relatively simple configurations of brane locations and Wilson lines) yield gauge groups that cannot directly provide a $SU(3)_{color}$ candidate (see, e.g., [9,27] and references therein). In addition, most of the $U(1)$ factors were anomalous and therefore massive, leading to a generic difficulty in obtaining $U(1)_Y$-hypercharge candidates for the standard model [27]. The particular $\mathbf{Z_6}$ orientifold, explored in this paper, could potentially provide the candidate group structure for both $SU(3)_{color}$ as well as non-anomalous $U(1)_Y$. The latter motivation was originally based on the observation [18] that branes at *orbifold* points, which are not fixed under the orientifold projection, may allow for appearance of non-anomalous $U(1)$'s, that could play the role of hypercharge.

The systematic exploration of N=1 supersymmetric discrete Wilson line solutions yields a surprisingly small number of non-equivalent classes of models. This result is due to the extremely tight tadpole consistency conditions for N=1 supersymmetric models, as well as the large symmetry group of the underlying geometry $T^6/\mathbf{Z_6}$, which we exploit extensively to identify different equivalence classes. In particular, N=1 supersymmetry constraints do not allow us to locate six (or more) branes at the $\mathbf{Z_3}$ orbifold points and obtain realistic gauge structure from these D3 branes in the model, even though this is a configuration that has the potential for yielding three-family sectors with the standard model (or left-right symmetric) gauge group. However, as we demonstrated in subsection V C, such configurations are possible if one allows for the introduction of anti-branes in the model, which lead to the breakdown of supersymmetry in the anti-brane sector.

The upshot of the exploration of N=1 supersymmetric models, which contain sectors with $SU(3)$ as a $SU(3)_{color}$ candidate, is the existence of only two inequivalent classes of

such solutions. We provide the complete spectrum and trilinear superpotential couplings for one class (the second equivalence class would yield an equivalent "observable sector" gauge group and spectrum). The model allows for the gauge group assignment: $SU(3)_{color} \times SU(2)_L \times SU(2)_R \times U(1)_{B-L}$, with the non-Abelian part arising from branes located at the $\mathbf{Z_6}$ orbifold fixed point. Interestingly, the non-anomalous Abelian factor $U(1)_{B-L}$ is however a combination of $U(1)$ factors arising from different sets of branes, namely D3- and D7-branes. Unfortunately, the above particular gauge group assignment has a major flaw, since it leads to only two sets of quark families. Nevertheless, other observable sector gauge group assignments are possible, and a more general phenomenological exploration of this model is under way [19].

ACKNOWLEDGMENTS

We would like to thank P. Langacker for many discussions, suggestions regarding the manuscript and for collaboration on related topics. We also benefited from discussions with G. Aldazabal, L. E. Ibáñez, M. Plümacher, F. Quevedo and R. Rabadán. We would like to thank SISSA, Trieste, Italy (M.C.) CAMTP, Maribor, Slovenia (M.C.), the Department of Physics and Astronomy, Rutgers University (M.C.), the Department of Physics and Astronomy of the University of Pennsylvania (A.U., J.W.), and the Centro Atómico Bariloche, Argentina (A.U.) for support and hospitality during the completion of the work. The work was supported in part by U.S. Department of Energy Grant No. DOE-EY-76-02-3071 (M.C.), in part by the University of Pennsylvania Research Foundation award (M.C.) and the NATO Linkage grant 97061 (M.C.). J.W. is supported by Department of Energy Grant No. DE-AC02-76CH03000.

REFERENCES

[1] C. Angelantonj, M. Bianchi, G. Pradisi, A. Sagnotti and Ya.S. Stanev, Phys. Lett. B385 (1996) 96, hep-th/9606169.

[2] M. Berkooz and R.G. Leigh, Nucl. Phys. B483 (1997) 187, hep-th/9605049.

[3] G. Zwart, Nucl. Phys. B526 (1998) 378, hep-th/9708040; Z. Kakushadze, Nucl. Phys. B512 (1998) 221, hep-th/9704059; Z. Kakushadze and G. Shiu, Phys. Rev. D56 (1997) 3686, hep-th/9705163; D. O'Driscoll, hep-th/9801114.

[4] Z. Kakushadze and G. Shiu, Nucl. Phys. B520 (1998) 75, hep-th/9706051.

[5] L. Ibáñez, *JHEP* **9807** (1998) 002, hep-th/9802103.

[6] G. Aldazabal, A. Font, L.E. Ibáñez and G. Violero, Nucl. Phys. B536 (1999) 29, hep-th/9804026.

[7] Z. Kakushadze and S.H.H. Tye, Phys. Rev. D58 (1998) 126001, hep-th/9806143; G. Shiu and S.H.H. Tye, Phys. Rev. D58 (1998) 106007, hep-th/9805157.

[8] Z. Kakushadze, Phys. Lett. B434 (1998) 269, hep-th/9804110; Phys. Rev. D58 (1998) 101901, hep-th/9806044; Nucl. Phys. B535 (1998) 311, hep-th/9806008.

[9] M. Cvetič, M. Plümacher and J. Wang, *JHEP* **0004** (2000) 004, hep-th/9911021.

[10] For examples of orientifolds of type IIB orientifolds non-geometric (asymmetric) orbifolds, see
M. Bianchi, J. F. Morales and G. Pradisi, Nucl. Phys. B573 (2000) 314, hep-th/9910228; R. Blumenhagen, L. Görlich, B. Körs and D. Lüst, Nucl. Phys. B582 (2000) 44, hep-th/0003024.

[11] G. Cleaver, M. Cvetič, J. R. Espinosa, L. Everett, and P. Langacker, Nucl. Phys. **B525** (1998) 3, hep-ph/9711178 and Nucl. Phys. **B545** (1999) 47, hep-th/9805133.

[12] M. R. Douglas, B. R. Greene and D. R. Morrison, Nucl. Phys. **B506** (1997) 84, hep-th/9704151; D. R. Morrison and M. R. Plesser, Adv. Theor. Math. Phys. **3** (1999) 1, hep-th/9810201; C. Beasley, B. R. Greene, C. I. Lazaroiu and M. R. Plesser, Nucl. Phys. **B566** (2000) 599, hep-th/9907186.

[13] M. Cvetič, L. Everett, P. Langacker and J. Wang, *JHEP* **9904** (1999) 020, hep-th/9903051.

[14] J. Park, R. Rabadán and A. M. Uranga, Nucl. Phys. **B570** (2000) 38, hep-th/9907086.

[15] M. Cvetič and L. Dixon, unpublished; M. Cvetič, in Proceedings of *Superstrings, Cosmology and Composite Structures*, College Park, Maryland, March 1987, S.J. Gates and R. Mohapatra, eds. (World Scientific, Singapore, 1987), Phys. Rev. Lett. **59** (1987) 1795, and Phys. Rev. Lett. **59** (1987) 2829.

[16] J. Lykken, E. Poppitz and S. P. Trivedi, Nucl. Phys. **B543** (1999) 105, hep-th/9806080.

[17] M. Cvetič and P. Langacker, Nucl. Phys. **B586** (2000) 287, hep-th/0006049.

[18] G. Aldazabal, L. E. Ibanez, F. Quevedo and A. M. Uranga, hep-th/0005067.

[19] M. Cvetič, P. Langacker, A.M. Uranga and J. Wang, work in progress.

[20] L.E. Ibáñez, R. Rabadán and A.M. Uranga, Nucl. Phys. B542 (1999) 112, hep-th/9808139.

[21] G. Aldazabal, D. Badagnani, L. E. Ibanez and A. M. Uranga, 'Tadpole versus anomaly cancellation in D = 4, D = 6 compact IIB orientifolds', *JHEP* **9906** (1999) 31, hep-th/9904071.

[22] A. Sagnotti, Phys. Lett. B294 (1992)196, hep-th/9210127.

[23] E. Poppitz, Nucl. Phys. B542 (1999) 31, hep-th/9810010.

[24] G. Aldazabal, L. E. Ibáñez and F. Quevedo, *JHEP* **0001** (2000) 031, hep-th/9909172; hep-ph/0001083.

[25] I. Antoniadis, E. Dudas and A. Sagnotti, Phys. Lett. **B464** (1999) 38, hep-th/9908023; G. Aldazabal and A. M. Uranga, *JHEP* **9910** (1999) 024, hep-th/9908072.

[26] C. Angelantonj, I. Antoniadis, G. D'Appollonio, E. Dudas and A. Sagnotti, Nucl. Phys. **B572** (2000) 36, hep-th/9911081; C. Angelantonj, R. Blumenhagen and M. R. Gaberdiel, hep-th/0006033; R. Rabadán and A. M. Uranga, hep-th/0009135.

[27] P. Langacker, private communications.

Appendix: T-duality and Fourier transformation of tadpole conditions

In this Appendix we show that tadpole cancellation conditions of orientifold models related by T-duality are related by a discrete Fourier-transform. The basic motivation for the proposal is that T-duality maps twisted sectors of one model to linear combinations of twisted sectors in the T-dual, with coefficients defining precisely a discrete Fourier transform. Hence orientifold twisted charges in a model and its T-dual must be related by such a discrete Fourier transform. Finally, consistent coupling of D-branes to twisted fields in a model and its T-dual implies that D-brane twisted charges, e.g., their contribution to twisted tadpoles, must also be related in this way.

In order to be concrete, we focus on the specific example of the $T^6/\mathbf{Z_3}$ orientifold, even though the technique is valid in general. Let us consider a $T^6/\mathbf{Z_3}$ type IIB orbifold modded out by Ω [1], and let us introduce general order three Wilson lines along the three complex planes and acting on the D9-branes through matrices $\gamma_{W_i,9}$. The twisted tadpole conditions at a θ-fixed point, generally denoted (m_1, m_2, m_3), with $m_i = 0, \pm 1$, read

$$\begin{array}{ll} (m_1, m_2, m_3) & \mathrm{Tr}\,(\gamma_{\theta,9}\gamma_{W_1,9}^{m_1}\gamma_{W_2,9}^{m_2}\gamma_{W_3,9}^{m_3}) = -4\ ; \\ & \mathrm{Tr}\,(\gamma_{\theta^2,9}\gamma_{W_1,9}^{2m_1}\gamma_{W_2,9}^{2m_2}\gamma_{W_3,9}^{2m_3}) = -4\ . \end{array} \tag{83}$$

It is convenient to make them a bit more explicit. Since all matrices commute and are of order three, they can be diagonalized, with eigenvalues $1, e^{2\pi i/3}, e^{2\pi i\frac{2}{3}}$. Let us denote by n_{r,s_1,s_2,s_3} the number of entries with eigenvalues $e^{2\pi i r/3}$, $e^{2\pi i s_a/3}$, in $\gamma_{\theta,9}$, $\gamma_{W_a,9}$, respectively. The tadpole conditions read

$$\begin{array}{ll} (m_1, m_2, m_3) & \sum_{r,s_1,s_2,s_3} e^{2\pi i r/3} e^{2\pi i\, m_1 s_1/3} e^{2\pi i\, m_2 s_2/3} e^{2\pi i\, m_3 s_3/3} n_{r,s_1,s_2,s_3} = -4\ ; \\ & \sum_{r,s_1,s_2,s_3} e^{2\pi i\, 2r/3} e^{2\pi i\, 2m_1 s_1/3} e^{2\pi i\, 2m_2 s_2/3} e^{2\pi i\, 2m_3 s_3/3} n_{r,s_1,s_2,s_3} = -4\ . \end{array} \tag{84}$$

Performing a T-duality along all compact directions, we get a $T^6/\mathbf{Z_3}$ type IIB orbifold modded out by $\Omega(-1)^{F_L}R$, where R reflects all internal dimensions (see [16] for a detailed description of this model). This T-dual model contains D3′-branes (we use primes to denote D-branes in the T-dual picture) which are located at the 27 θ-fixed points, denoted (t_1, t_2, t_3), $t_a = 0, \pm 1$. By the usual T-duality correspondence between Wilson line eigenvalues and D-brane positions, D9-branes with Wilson line eigenvalues defined by s_i map to D3′-branes sitting at $(t_1, t_2, t_3) = (s_1, s_2, s_3)$, hence $\gamma_{\theta,3,(t_1,t_2,t_3)}$ has n_{r,t_1,t_2,t_3} eigenvalues $e^{2\pi i r/3}$. This completely specifies the T-dual model in terms of the original one.

Our purpose now is to perform the discrete Fourier transform in the tadpole cancellation conditions (84), and show that they correspond to the tadpole cancellation conditions in the T-dual description. For instance, for the θ-twisted tadpole equation, multiplying the first equation in (84) by $e^{-2\pi i\, m_1 t_1/3} e^{-2\pi i\, m_2 t_2/3} e^{-2\pi i\, m_3 t_3/3}$ and summing over m_1, m_2, m_3, we get

$$27 \sum_{r,s_1,s_2,s_3} e^{2\pi i r/3} \delta_{s_1,t_1} \delta_{s_2,t_2} \delta_{s_3,t_3} n_{r,s_1,s_2,s_3} = -4 \times 27 \times \delta_{t_1,0} \delta_{t_2,0} \delta_{t_3,0} \ . \tag{85}$$

Summing over s_1, s_2, s_3 we get

$$\sum_r e^{2\pi i r/3} n_{r,t_1,t_2,t_3} = -4 \delta_{(t_1,t_2,t_3),(0,0,0)} \ . \tag{86}$$

Recalling the T-dual interpretation of n_{r,t_1,t_2,t_3} as multiplicities in $\gamma_{\theta,3',(t_1,t_2,t_3)}$, we obtain

$$\mathrm{Tr}\, \gamma_{\theta,3',(t_1,t_2,t_3)} = -4 \delta_{(t_1,t_2,t_3),(0,0,0)} \ . \tag{87}$$

These are precisely the θ-twisted tadpole conditions in the T-dual model [16], i.e. the $\Omega R (-)^{F_L}$ orientifold of $T^6/\mathbf{Z_3}$. Namely the origin is fixed under the orientifold action and receives a crosscap contribution equal to -4, while the remaining points are not fixed under the orientifold action, and do not have such contribution. Clearly, one can repeat the exercise for θ^2, leading to the analogous result.

To show the technique is completely general, let us repeat the exercise for the $\mathbf{Z_6}$ orientifold and its T-dual along the first two complex planes, which is itself a $\mathbf{Z_6}$ orientifold with D9- and D5$_3$-branes mapping to D5$'_3$- and D9-branes.

We consider a quite general configuration with D9-branes with order three Wilson lines along all three complex planes, and D5$_3$ branes sitting at different θ^2-fixed points in the first and second plane, and with order three Wilson lines on the third. The tadpole conditions are given in (32). Let us concentrate on those associated with θ^2, which can be condensed as

$$(m_1, m_2, m_3): \ \mathrm{Tr}\, (\gamma_{\theta^2,9} \gamma_{W_1,9}^{m_1} \gamma_{W_2,9}^{m_2} \gamma_{W_3,9}^{2m_3}) \ + 3 \mathrm{Tr}\, (\gamma_{\theta^2,5,(m_1,m_2)} \gamma_{W_3,5_3,(m_1,m_2)}^{2m_3}) = 12 \delta_{m_1,0} \delta_{m_2,0} + 4 \ . \tag{88}$$

The order three Wilson lines along the first complex plane have the structure determined in Subsection IIA. In particular they commute with $\gamma_{\theta^2,9}$ and among themselves (and so does $\gamma_{W_3,9}$), so we may diagonalize them simultaneously. Let us denote by n_{r,s_1,s_2,s_3} the number of eigenvalues $e^{2\pi i r/3}$, $e^{2\pi i s_a/3}$, in $\gamma_{\theta^2,9}$, $\gamma_{W_a,9}$, respectively. The matrix $\gamma_{W_3,5_5,(m_1,m_2)}$ also commutes with $\gamma_{\theta^2,5_3,(m_1,m_2)}$, and we may diagonalize these as well. Let us denote by $m_{r m_1 m_2 s_3}$ the number of eigenvalues $e^{2\pi i r/3}$, $e^{2\pi i s_3/3}$ in $\gamma_{\theta^2,5_3,(m_1,m_2)}$, $\gamma_{W_3,5_3,(m_1,m_2)}$, respectively.

Clearly, after T-dualizing along the first two complex planes D9-branes with W_1, W_2 Wilson line eigenvalues determined by s_1, s_2 are mapped to D5$'_3$-branes sitting at the point (s_1, s_2). Similarly, D5$_3$-branes at (m_1, m_2) map to D9$'$-branes with W_1, W_2 Wilson line eigenvalues determined by m_1, m_2. Hence, in the T-dual picture $n_{r s_1 s_2 s_3}$ denotes the number of entries with eigenvalues $e^{2\pi i r/3}$, $e^{2\pi i s_3/3}$ in $\gamma_{\theta^2,5'_3,(s_1,s_2)}$, $\gamma_{W_3,5'_3,(s_1,s_2)}$, respectively, and

$m_{rm_1m_2s_3}$ denotes the number of entries with eigenvalues $e^{2\pi ir/3}$, $e^{2\pi im_1/3}$, $e^{2\pi im_2/3}$, $e^{2\pi is_3/3}$ in $\gamma_{\theta^2,9'}$, $\gamma_{W_a,9'}$, respectively. This completely specifies the T-dual model. Our purpose, in what follows, is to show that the consistency conditions in the original model, after the discrete Fourier transform, provide the consistency conditions in the T-dual picture.

The tadpole condition (88) reads

$$\sum_{r,s_1,s_2,s_3} e^{2\pi i\frac{r}{3}} e^{2\pi i\frac{m_1s_1}{3}} e^{2\pi i\frac{m_2s_2}{3}} e^{2\pi i\frac{2m_3s_3}{3}} n_{rs_1s_2s_3} + 3\sum_{r,s_3} e^{2\pi i\frac{r}{3}} e^{2\pi i\,\frac{2m_3s_3}{3}} m_{rm_1m_2m_3} = \\ = 12\delta_{m_1,0}\delta_{m_2,0} + 4\,. \tag{89}$$

Multiplying by $e^{-2\pi i\, m_1t_1/3} e^{-2\pi i\, m_2t_2/3}$ and summing over m_1, m_2, we get

$$9\sum_{r,s_1,s_2,s_3}\; e^{2\pi i\frac{r}{3}}\;\delta_{s_1,t_1}\;\delta_{s_2,t_2}\; e^{2\pi i\frac{2m_3s_3}{3}} n_{rs_1s_2s_3} + \\ + 3\sum_{rm_3} e^{2\pi i\frac{r}{3}}\; e^{-2\pi i\frac{m_1t_1}{3}}\; e^{-2\pi i\frac{m_2t_2}{3}}\; e^{2\pi i\frac{2m_3s_3}{3}}\; m_{rm_1m_2m_3} = 12 + 36\,\delta_{t_1,0}\delta_{t_2,0}\,.$$

Summing over s_1, s_2 we get

$$\sum_{r,m_1,m_2,m_3} e^{2\pi i\frac{r}{3}}\; e^{-2\pi i\frac{m_1t_1}{3}}\; e^{-2\pi i\frac{m_2t_2}{3}}\; e^{2\pi i\frac{2m_3s_3}{3}}\; m_{rm_1m_2m_3} + \\ + 3\sum_{r,m_3} e^{2\pi ir/3}\; e^{2\pi i\,2m_3s_3/3}\; n_{rt_1t_2m_3} = 12\,\delta_{t_1,0}\,\delta_{t_2,0} + 4\,. \tag{90}$$

Now, using the T-dual interpretation of $n_{rt_1t_2s_3}$ and $m_{rm_1m_2m_3}$, we finally obtain

$$\mathrm{Tr}\,(\gamma_{\theta^2,9'}\gamma^{t_1}_{W_1,9'}\gamma^{t_2}_{W_2,9'}\gamma^{2s_3}_{W_3,9'}) + 3\mathrm{Tr}\,(\gamma_{\theta^2,5'_3,(t_1,t_2)}\gamma^{2s_3}_{W_3,5'_3,(t_1,t_2)}) \;=\; 12\delta_{(t_1,t_2),(0,0)} + 4\,, \tag{91}$$

which is precisely the θ^2 tadpole condition at the point (t_1, t_2, s_3), which is of the form (88) since the T-dual picture is again an Ω orientifold of $T^6/\mathbf{Z_6}$.

Notice that the T-duality discussed for the $\mathbf{Z_6}$ orientifold in Section III is along the third complex plane, therefore it is identical to that performed for the $\mathbf{Z_3}$ orientifold in this Appendix (and differs from that studied here for the $\mathbf{Z_6}$ case).